FACULTY OF SCIENCE
UNIVERSITY OF COPENHAGEN

THE CORRELATION BETWEEN CRITICAL ANAESTHETIC DOSE AND MELTING TEMPERATURES IN SYNTHETIC MEMBRANES

With comments on the possible implications of the soliton model on epilepsy

Fatma Tounsi

Supervisor: Thomas Heimburg

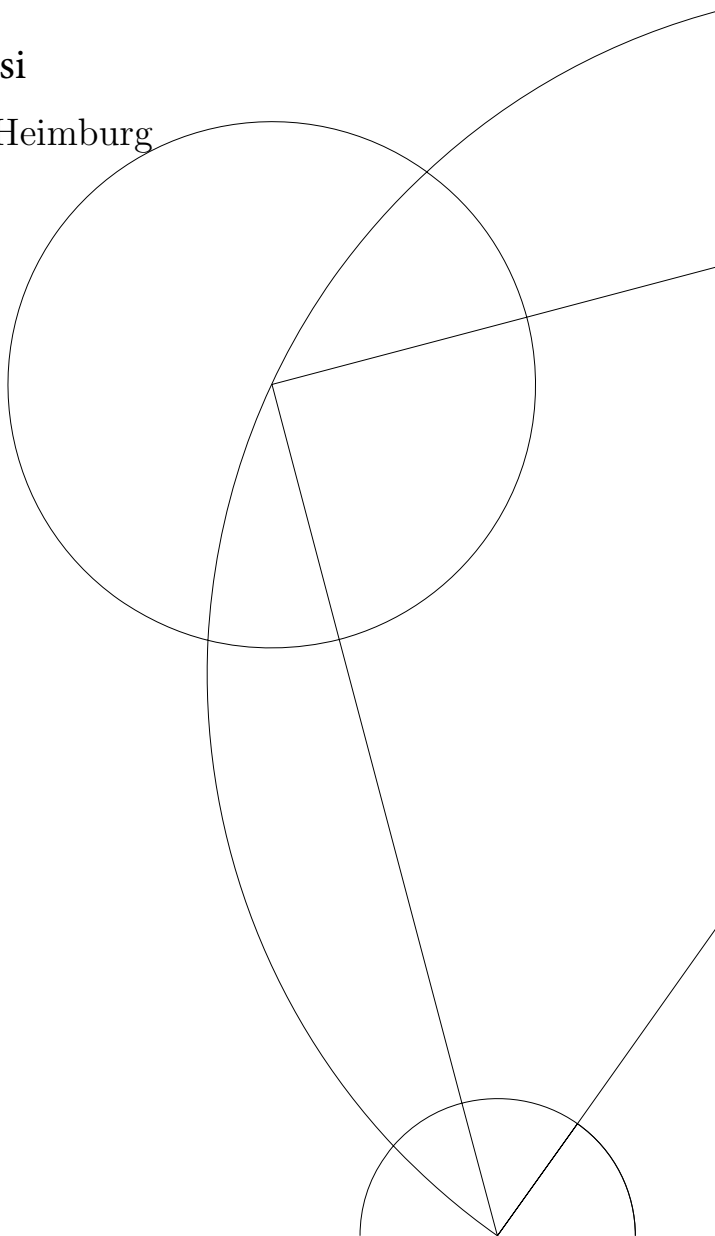

A Thesis Presented for the Degree of
Cand. Scient. in Biochemistry

Niels Bohr Institute
University of Copenhagen

November 25, 2015

O soothest Sleep! if so it please thee, close
In midst of this thine hymn my willing eyes,
Or wait the "Amen," ere thy poppy throws
Around my bed its lulling charities.
Then save me, or the passed day will shine
Upon my pillow, breeding many woes,—
Save me from curious Conscience, that still lords
Its strength for darkness, burrowing like a mole;
Turn the key deftly in the oiled wards,
And seal the hushed Casket of my Soul.

John Keats

ACKNOWLEDGMENTS

I would like to thank Henrike Sasse-Middelhoff for her thorough and patient introduction to the laboratory and for her subsequent help with questions.

A big thank you to Karis Zecchi for always being helpful in the laboratory as well as with questions.

Thanks to Tian Wang for the numerous interesting discussions we had in the office, and for her great help with the nerve experiments, in hope of their continual very soon.

Thanks to Lars and Alfredo for their conversation and advise.

A very grateful thank to my supervisor Thomas Heimburg for taking a biochemist into the fantastic world of biophysics and for allowing me to be ambitious despite my humble abilities.

Last but not least, many thanks to my dear family for supporting me through the stress and turmoil of the last few months and especially the last of weeks of the writing process.

ABSTRACT

The anaesthetic potency of a substance is closely related to its lipophilicty. This has been interpreted as evidence for a lipid mechanism of action for anaesthesia. However, with the success of the conductance based Hodgkin-Huxley model for the nerve impulse, the scientific community shifted to considering protein ion-channels the cellular target for anaesthetics. Today, the lipid hypothesis has returned with a mechanism of action based on a whole new view of the nerve impulse as a theromodynamic event rather than an electric one. The new model is known as the soliton model, because it describes the nerve impulse as a solitary density wave.

In this project we find that the soliton model can explain the cut-off of anaesthetic potency in n-alkanes. Then we consider the medical implications that the soliton might have for the neurological desease, epilepsy.

TABLE OF CONTENTS

PREFACE

Every day hundreds of thousands of people are anaesthetised around the globe, yet anaesthesia remains one of the black boxes of modern science. If there is a single fact that we know about anaesthetics without doubt, it is that their potency is correlated to their solubility in the lipid membrane. Yet, we cannot always tell what is going to be an anaesthetic and what is not. Some substances look like known anaesthetics and do dissolve in the lipid membrane, but are not anaesthetic. The most famous case of this is the long chain alcohols and alkanes, that unlike the shorter members of these homolgous groups do not have an anaesthetic effect.

In 2004, Thomas Heimburg and Andrew Jackson suggested a model that not only explains how anaesthesia works and why the long chained carbohydrates are not anaesthetic like their mates; it also explains other perviously puzzling phenomena such as the reversible heat production and the mechanical changes that can be measured during the nerve impulse. The trick is, that we have to change our entire view on how nerves work in order to explain these phenomena and many others that the electricity-centric ion channel model cannot explain.

The first two chapters of this project will try to give an overview of the experimental and theoretical work that took place over the last century and a half and how our view of aneasthesia, cell membranes and nerves developed through the years untill we reach the soliton model, which Heimburg and Jackson suggest. Then we will look at one of the exceptional cases in the lipophilicity-potency correlation and investigate whether the new model does indeed explain this case.

In the latter part of the project, we shift gears, and look at the consequences the soliton model can have for neurological diseases, sepcifically epilepsy. The reason we chose to look at epilepsy rather than other disorders is the close relation between it and anaesthesia, as we will try to show. This part of the project is somewhat accidental; a curious result of the distractibility of the author. We will not be able to reach any conclusions or answer any questions but will hopefully open the door for many questions more.

CHAPTER 1

AN INTRODUCTION TO ANAESTHESIA

1.1 A historical background

Since antiquity, humans have subjected themselves to the horrific, excruciating pain of surgery in pursuit of survival. The pain, together with the dangers of bleeding and infection, made the incision tools a very last resort. Surgical procedures were, for the greatest part of human history, mostly restricted to amputations and tumour removal.

Several ancient civilizations have recorded the use of certain substances to induce analgesia and sedation during surgery. The most noteworthy and widespread were alcohol, opiates extracted from poppy seeds and hashish. Yet, it is only in the 19th century that anaesthetics were discovered; and together with the concurrent discovery of antisepsis, this allowed for the launch of modern surgery.

The discovery of anaesthesia can be traced back to Humphry Davy, a chemist and physicist, who in 1800 published a treatise, a significant part of which was dedicated to describing the "new and peculiar sensations" experienced by him and several of his friends when inhaling nitrous oxide. Having noticed the analgesic effect of the gas, the twenty-year-old Davy suggested in his treatise that it might be useful in operations (Davy 1800). Not being a physician himself, however, he had to relinquish the honour of the first use of an anaesthetic in surgery to another. So for a while, nitrous gas was restricted to recreational use and exhibitions for entertaining the public.

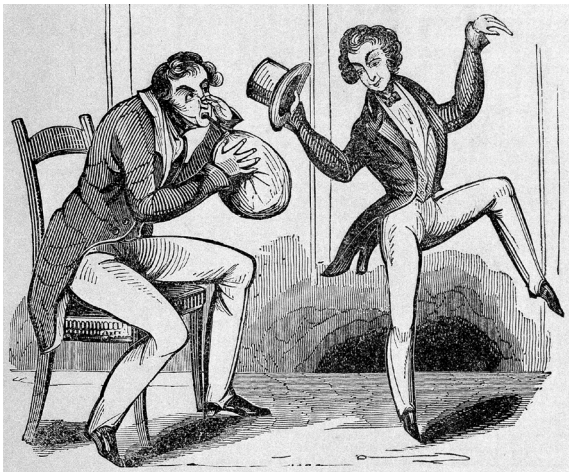

Figure 1: A satirical illustration taken from a poster advertising an "Exhibition of the laughing gas" from the 1840s. (Wikimedia Commons).

Forty two years later on a different continent, Crawford W. Long, observed the recreational use of diethyl ether noticing that it had similar effects to those Davy described for nitrous oxide. On the 30th of March 1842, Long conducted the first trial in which he used ether during the removal of a tumour, and later used it for amputations and child

birth. By the end of the century, three different anaesthetics were in use; nitrous oxide, anaesthesia and chloroform, and the tortured shrieks of the operation room were finally silenced.

1.2 What is anaesthesia?

General anaesthetics are used to ensure that patients are not conscious during surgical procedures and do not produce any reflexes in response to surgical incision. A general anaesthetic is commonly defined as a substance that can reversibly induce loss of consciousness. However, since consciousness is difficult to define and is yet impossible to measure, anaesthesia is more practically defined as a state of unresponsiveness to stimulus (Shafer 2008). It is important to specify the functional endpoint used to determine whether anaesthesia is achieved, as it is not an all-or-none phenomenon, but a progressive continuum of states (Roth 1979). While an unconscious patient might not respond to benign stimulus such as their name being called, they could be roused back to consciousness by a noxious stimulus such as surgical incision.

The continuum of anaesthetic effect starts with drowsiness and impairment of cognition followed by hyperexcitation. As the dose is increased, a state of conscious sedation, known clinically as twilight anaesthesia, is reached. At this stage, activity and alertness are decreased and the ability to form new memories is impaired (anterograde amnesia) (Perouansky 2014). Finally, a state of unconsciousness is entered which as mentioned above, varies in depth (Little 1996).

Anaesthetics do not affect the nervous system alone. In fact, they affect most, if not all, physiological systems, most notably, the cardiovascular and respiratory systems (Perouansky 2014). These effects vary from one drug to the other. For example, while halothane causes hypotension, ketamine raises the blood pressure.

It should also be noted that the effect of anaesthetics on the sensation of pain before loss of consciousness is not a uniform one. As mentioned earlier, the analgesic effect of ether and nitrous oxide played a key role in the discovery of anaesthesia, however not all anaesthetics share this property, for example, Benzodiazepines are not analgesics. On the other hand, some drugs such as opiates produce analgesia without being able to produce anaesthesia, although they do have a sedative effect. Neuromuscular blockers produce immobility without affecting consciousness (Little 1996). They are sometimes used in combination with general anaesthetics, thus making the task of evaluating the patient's consciousness, which depends greatly on the expertise of trained anaesthesiologists, an even trickier one. The anaesthetic dose needed for a patient is affected by many factors such as age, height, weight, body temperature, and alcohol and drug use.

Figure 2 shows a number of anaesthetics that are currently used clinically, in addition to diethyl ether, chloroform, and cyclopropane which are no longer in use due to flammability, toxicity and side effects, respectively. As the figure clearly shows, anaesthetics vary greatly in their chemical structures. Inhaled anaesthetics include xenon, a noble gas, Nitrous oxide, an inorganic gas, and halogenated hydrocarbons. Intravenous anaesthetics include barbiturates and benzodiazepines in addition to others. This is not all. Hundreds of substances have been found to possess anaesthetic effect when tested on model organisms in the lab (Urban 2008). These include noble gasses, diatomic gasses such as nitrogen, inorganic gasses such as CO2, alcohols, alkanes, ketones, and many more. Despite their varying structures, the anaesthetic effect of these substances is additive (Overton 1901).

When applied directly to nerves, anaesthetics are thought to block the nerve impulse (Seeman 1972); however a very recent study indicates that they merely change the stimulus vs. impulse behaviour. We will discuss this result and its implications further in the next chapter.

1.3 The universality of anaesthesia

Historically, the discovery of anaesthetics is an important one because of their utility in surgical operations. Therefore, their effect on consciousness remains the centre of focus. However, the effect of anaesthetics is so universal that it encompasses not only any organism with a nervous system, but also non-neuronal cells and even yeast and bacteria. Most notable is their effect on cell permeability and on haemolysis.

In researching the effect of anaesthesia, a number of model organisms have been used. As with almost any other area of biological or medical research, mice are often used to research anaesthesia. The end-point used to determine the occurrence of anaesthesia in them is loss of righting reflex. Alternatively, a tail clamp may be used. Tadpoles were probably the first model organism to be used in anaesthesia research, and are still used today. When anesthetized they stop swimming, sink to the bottom, and lose their startle reflex. Other organisms that are used in anaesthesia reserch are Zebra fish, fruit flies, and C. Elegans. In studies about the nerve blocking properties of anaesthetics, we find the usual suspects of neurophysiology research; squids, lobsters, frogs, and earthworms.

1.4 Measuring aesthetic potency

Since most clinically used anaesthetics are volatile, the most prevalent measurement of aesthetic potency is the minimum alveolar concentration (MAC). It is obtained from a dose-response curve (see Figure 3), in which the percent of patients is plotted against log of the alveolar concentration of the drug, i.e. the end-tidal concentration. MAC is the concentration at which 50% of patients are anesthetised, thus, it is actually a median not a minimum (Urban 2008).

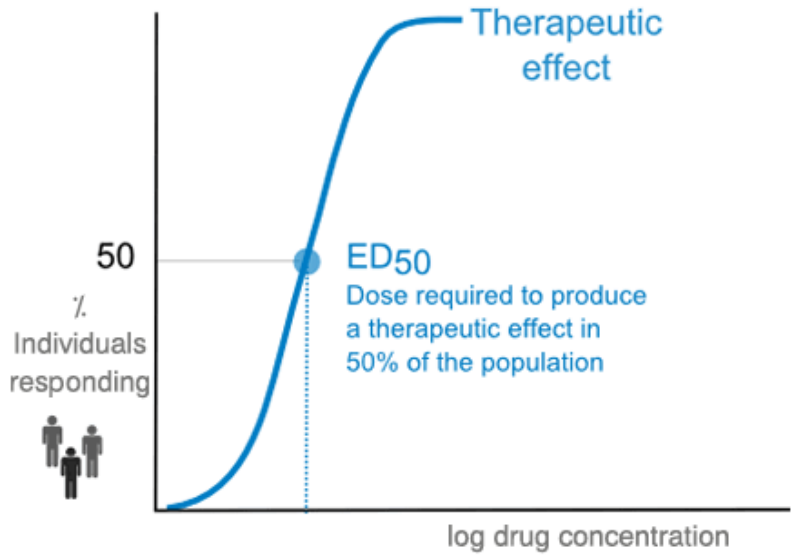

Figure 3: A schematic of a drug response curve (pharmacologycorner.com)

As we mentioned earlier, it is important to specify the functional end-point used to determine the state of anaesthesia, as the anaesthetic dose differs for different end-points. In medical studies, the end-point is lack of response to incision. For intravenous anaesthetics, the corresponding value is CP_{50}: the plasma concentration at which 50% of patients are anesthetised (Urban 2008). A less useful measurement is ED_{50}, median effective dose, as it does not take into account the change of concentration due to metabolism.

In the lab, EP_{50} (median effective partial pressure) is used for volatile anaesthetics, while EC_{50} is used when anaesthetics are dissolved in the aquatic environment of tadpoles and zebra fish (Urban 2008).

The dose-response curve for anaesthesia is a steep one, thus that it only takes a dose 10-20% higher than MAC to anaesthetise almost all patients (Pluzewski 1983).

CHAPTER 2:

THE SEARCH FOR A MECHANISM

Immediately after the discovery of anaesthetics, they became a hot topic for biological research. Very early on, they were linked to the lipid component of the cell, because of their lipid solubility which correlates tightly with anaesthetic potency. However, after the emergence of the Hodgkin-Huxley model, which describes the nerve impulse in terms of ion currents racing through selective, and time and voltage-dependent ion channels sitting in the plasma membrane, the protein "ion channels" became the preferred site of action for anaesthetics despite the lack of specific binding. Today, more than 150 years since anaesthetics entered the operation room, their cellular mechanism is still disputed.

In this chapter, we try to give an overview of scientific research and theories regarding anaesthesia, cell membranes and the mechanism behind nerve impulse propagation.

2.1 The Meyer-Overton rule and its "exceptions"

As a result of chloroform's and diethyl ether's ability to dissolve fats, anaesthesia was very early on linked to the fatty component of the cell, then known as lipoids. Another empirical observation that helped this idea on was the fact that the brain and spinal cord are especially rich in lipoids compared to other organs.

The existence of a semi-permeable membrane surrounding the cell had at this point been accepted, and it had also been suggested that this membrane consisted of a thin film of oil. This suggestion, made by physicist Georg Quincke who observed that an oil film acts as a semi-permeable membrane, was further supported by the research of Charles Overton, who found that substances that are more soluble in oil diffuse faster into the cell (Loeb 1904). It was not until 1924, however, that the lipid-bilayer cell membrane model was established.

Although initially interested in studying cell permeability, Overton is now mostly known for discovering the correlation between anaesthetic effect and lipophilicity. This correlation was discovered concurrently but independently by another scientist, phar-

macologist Hans Horst Meyer, thus it came to be known as the Meyer-Overton correlation. In his book, *Studies of Narcosis*, Overton states the correlation thus:

> *"… narcotic strength of a compound depends primarily upon its partition coefficient between the aqueous and lecithin-cholesterol related dissolving agents within the organism."*
>
> *(Overton 1901, p. 87 of the English edition)*

The partition coefficient is the ratio of concentrations of the un-ionized form of a substance in two immiscible phases. According to Nernst's distribution law, it is constant at constant temperatures. As a stand in for the cell lipoids, Overton used olive oil.

$$Partition\ Coefficient = \frac{[Solute]_{Oil}}{[Solute]_{Water}}$$

To measure the potency of anaesthetics Overton used tadpoles. He tested dozens of substances (reportedly, almost every commercially available chemical substance at the time) covering a great variety of chemical structures.

The Meyer-Overton correlation has since been tested on several species. Several organic solvents have been used to measure the partition coefficient, such as octanol, benzene and even phospholipid vesicles. Likewise, the aquous solvent can be a buffer. Alternatively the oil-water partition coefficient can be exchanged with the oil-gas one as shown in Figure 4. Moreover, many more anaesthetic substances have been found,

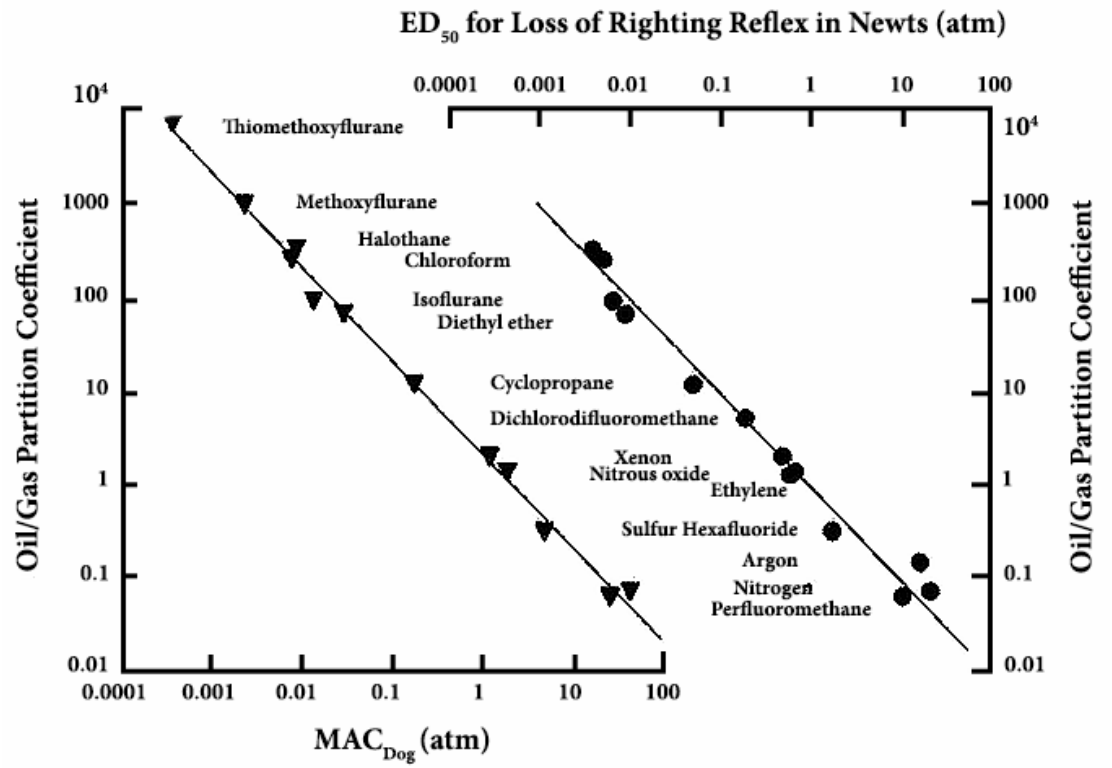

Figure 4: The Meyer Overton correlation as traditionally represented by plotting the partition coefficient against anesthetic potency. Here, data from dogs (triangles) and Newts (circles) are plotted simultaneously and each data set is fitted with a linear function (Reproduced from Antognini et al. 2003)

yet the correlation still holds true despite the genetic variance between the species, the structural variance of anaesthetics, and the fact that their partition coefficients span several degrees of order.

Meyer and Overton did not stop at establishing this empirical correlation but went on to formulate a hypothesis regarding anaesthetic mechanism of action. In *Studies of Narcosis*, Overton postulates:

> *"…that narcosis results from the modification (caused precisely by absorption of foreign compounds) of the normal physical states of lecithin and cholesterol compounds in the cell."*
>
> *(Overton 1901, p. 70 of of the English edition)*

The lipid hypothesis of anaesthetic action remained the backdrop, if not the focus, of this research area for the majority of the 20th century. Its biggest weakness has been the lack of a specific mechanism. Which physical state of the cell lipids do anaesthetics change? And how does this change affect the nerve function?

2.2 The "exceptions" to the Meyer-Overton rule

The lack of a specific mechanism of action was not the only obstacle that the Meyer-Overton hypothesis faced. Another was its inability to explain why some substances were not anaesthetic, while being perfectly capable of dissolving in the membrane, and even more, being structurally similar to some anaesthetic molecules. The most known case of this is the cut-off effect that occurs in homologous groups of hydrocarbon chains. As the number of carbon atoms increases in such a series, so does the partition coefficient. Accordingly the anaesthetic potency also increases but only up to a certain point, after which the potency is lower than is predicted by the partition coefficient. Then the anaesthetic potency disappears altogether for the longer chains. This effect was first noticed by Meyer and Overton in alcohols and alkanes, and has since then been a well known and well documented phenomenon.

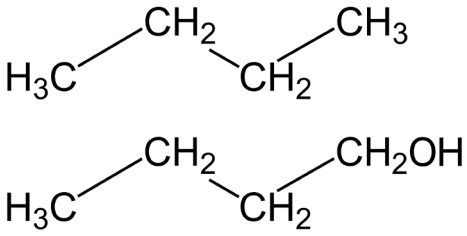

The fourth member of the n-alkane and 1-alkanol homologous series, n-butane and n-butanol respectively.

The length at which the cut-off happens is different from one series to another. For n-alcohols Meyer found that it happens at C13, which is completely inactive, while C14 is less potent than predicted (Meyer & Hemmi 1935). A later study also done on tadpoles found that C13 is weakly anaesthetic, while C14 does not induce anaesthesia (Pringle 1981).

A study done on C. Elegans showed that C9-C12 have a lower potency than expected, while C14 has a potency lower than shorter alcohols as shown inFigure 5. The study did not test longer n-alcohols. (Anton 1992).

n-alkanes were found to stop being anaesthetic at C11 in C. Elegans with the potency of C10 being lower than that of shorter alkanes, as shown in Figure 5 (Anton 1992) and in Drosophila melanogaster (Allada 1993). The nerve blocking ability of alkanes has also been shown to cut-off although at C9 rather than C 11 (Haydon 1977).

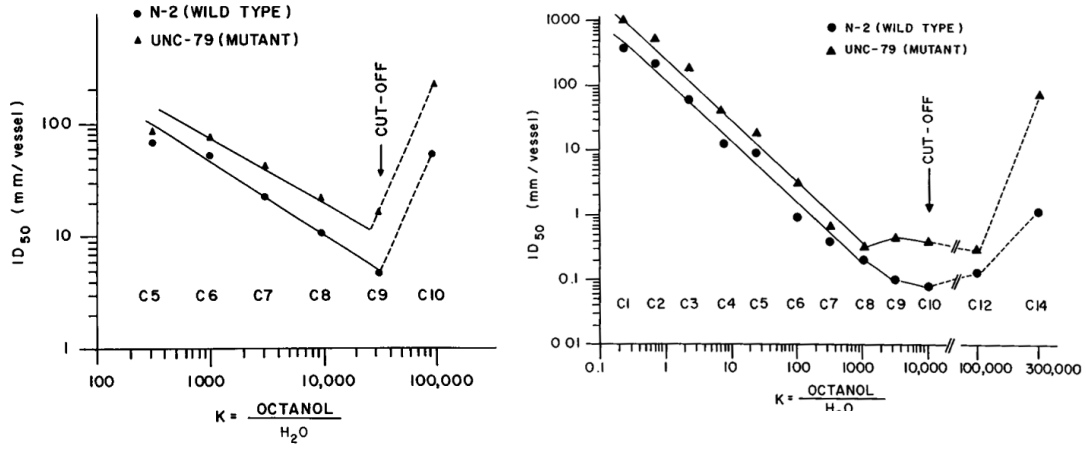

Figure 5: Median immobilising dose (ID50) of n-alkanes (left) and n-alkanols (right) measured in two C. Elegans strains and plotted against the water-octanol partition coeffitient. (Anton 1992)

The cut-off effect has also reported in tadpoles for 9-alken-1-ols at C8 for the cis isomers and at C9 for the trans isomers (Pringle 1981).

The long chain hydrocarbons are not the only substances expected to induce anaesthesia but fail to do so. Several fluorinated or halogenated compounds that are structurally related to anaesthetics but do not induce anaesthesia have been reported (Koblin 1994). Despite being lipid soluble, these compounds do not induce anesthesia, but instead produce tremors and convulsions. The most known among these compounds is Flurothyl, which is structurally related to diethyl ether and anaesthetic halogenated ethers. We will discuss flurothyl further in later chapters and will investigate its interaction with lipid vesicles.

Overton briefly discussed possible reasons behind the cut-off effect in alcohols. He explained it away with a decrease in the hydrocarbons' absolute solubility in the lipid. He does not clarify why this should be important, when the partition coefficient is definitely increasing and with it the molecule's concentration in the lipid phase. While Meyer and Overton were unable to find a satisfactory explanation for the cut-off effect, the answer lies hidden in the wording of their hypothesis. As we will go on to explain later in this chapter, a molecule must do more than adsorb into the membrane in order to induce anaesthesia; it must change its physical state. However, this would have been impossible to conjecture without the knowledge we have today about the nature of the biological membrane.

2.3 The plasma membrane – a fluid mosaic

The lipid bilayer structure of the plasma membrane was first deduced by Gorter and Grendel in 1925 through a rather simple experiment. Using a Langmuir trough, a devise that compresses lipid monolayers on a water surface, they found that the surface area of the lipids extracted from a red blood cell is about double the surface area of the cell. From this they concluded that the lipids must form a bilayer in the cell membrane. The ratio of areas was not precisely equal to two because of the presence of proteins, which they did not account for. The bimolecular structure was later confirmed by David Robertson through the use of electron microscopy (Heimburg 2007).

Lipids are small amphiphilic molecules that consist of a hydrophilic head, a hydrophobic tail, and a backbone that connects the two. The hydrophobic tail simply consists of one, two or three hydrocarbon chains which vary in length and in saturation. The head groups vary greatly in structure.

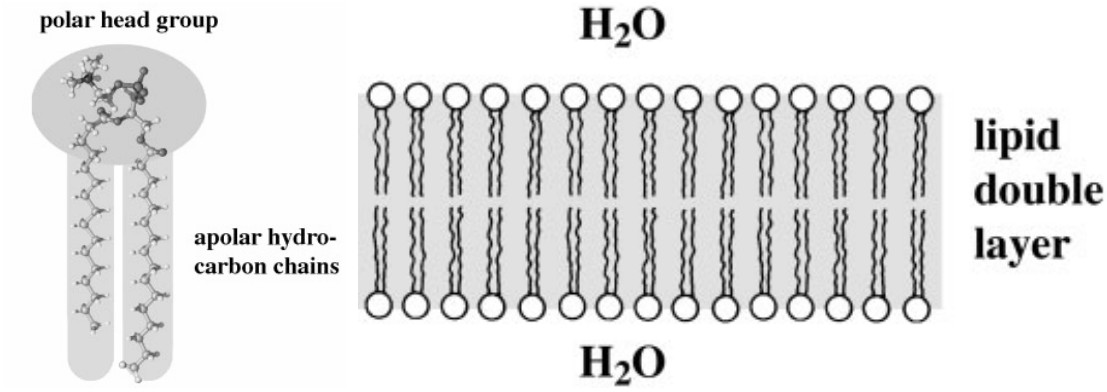

Figure 6: The chemical structure and amphiphilic nature of a phospholipid (Left). A schematic drawing of the lipid double layer structure know as the bilayer (right). (Heimburg 2007)

In water, lipids spontaneously aggregate forming many different structures depending on several variables such as the dimensions of the lipid molecules, the charge of the head group, the lipid's concentration in water and temperature and pressure. Common for all the different structures is that the hydrophilic parts always face the water, while the fatty hydrophobic parts face each other. One of these structures is the bilayer structure which we find in biological membranes.

Membrane lipid composition varies from species to species and from one cell type to the other. Most common are phospholipids, which have a negatively charged phosphate as a head group, a glycerol backbone, and two fatty acids in the tail. Of these the most common are phosphatidylcholines, which contain a choline in addition to phosphate in the head group. Other phospholipids include phosphatidylserine (PS) and phosphatidylethanolamine (PE).

Another important group of lipids is sphingolipids, which are especially prominent in the nervous system. In these lipids, one of the hydrocarbon tails is an amino alcohol,

known as a sphingosine, which also forms the backbone of the lipid. Sphingomyelin which consists of a sphingosine and a fatty acid is enriched in myelin sheaths. Cerebrosides are found in nerve and muscle cells, and have a single sugar as a head group. Gangliosides have large headgroups consisting of a oligosaccharide with one or more sialic acids, and are found in the nervous system.

Sterols are a major component of membranes, making up about 20% of its weight. Chorestol is the sterol found in animal cells. (Heimburg 2007)

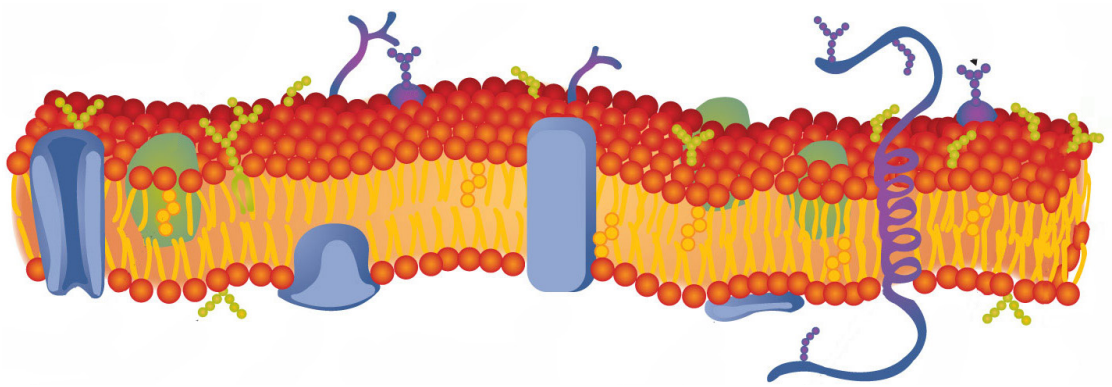

Figure 7: An artistic representation of the current view of the biological membrane

Proteins came into the picture later when x-ray crystallography revealed that membrane proteins have a high content of α-helices, which in turn contain many hydrophobic amino acids. From this it was concluded that proteins can span the membrane.

Later on, fluorescence labelling revealed that the membrane is not a static structure but a 2D fluid, in which lipids and proteins can diffuse freely (Frye & Edidin 1970). This gave way to the "fluid mosaic" model which today forms the basis for the scientific view of the cell membrane with some refinements; the formation of local domains that differ from their surroundings in lipid content and structure, the inhomogeneous distribution of lipids between the two leaflets, and variation in the lipid bilayer thickness to accommodate for the thickness of the hydrophobic region in transmembrane proteins (Heimburg 2007).

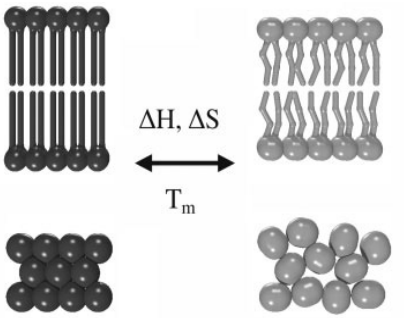

Figure 8: An illustration of the change in lipid structure from the solid-ordered to the liquid-ordered phase. Top: A side view showing the loss of order in the hydrocarbon chains. Bottom: A top view showing the loss of the crystalline order of the head groups. (Heimburg 2007)

Lipid bilayers can exist in a fluid liquid ordered phase or in a gel solid ordered phase. In the latter, the molecules are arranged in a lattice structure and have little mobility. The hydrocarbon chains exist in an all-trans conformation and are oriented perpendicularly to the plane of the bilayer. In the liquid order phase the average orientation of the chains is perpendicular to the plane, however their C-C trans-

fer rapidly and randomly between gauche and trans conformations. In this phase, molecules diffuse freely in the plane of the bilayer. The phase transition is energy consuming and brings a number of changes to the membrane properties. Its surface area and volume increase, while its thickness decreases as illustrated in Figure 8.

Since the phase transition involves adsorption or release of heat, it can be measured using a differential scanning calorimeter (DSC). This apparatus measures the heat added to amount of heat required to heat a sample, known as the heat capacity Cp. Outside a phase transition, Cp remains constant. When undergoing a transition from the gel to liquid phase, Cp increases then decreases again and finally goes back to constancy when all the lipid molecules have melted. When transitioning in the opposite direction, the process is exothermic rather than endothermic. The temperature at which Cp reaches a maximum (or minimum) is known as the melting temperature (T_m). Each lipid has a characteristic phase transition temperature and profile, although the latter depends on vesicle size and lamellarity. Figure 9. shows the phase transition profile of DPPC. Both Tm and phase transition profile can be changed by some factors such as pH, pressure, and solutes.

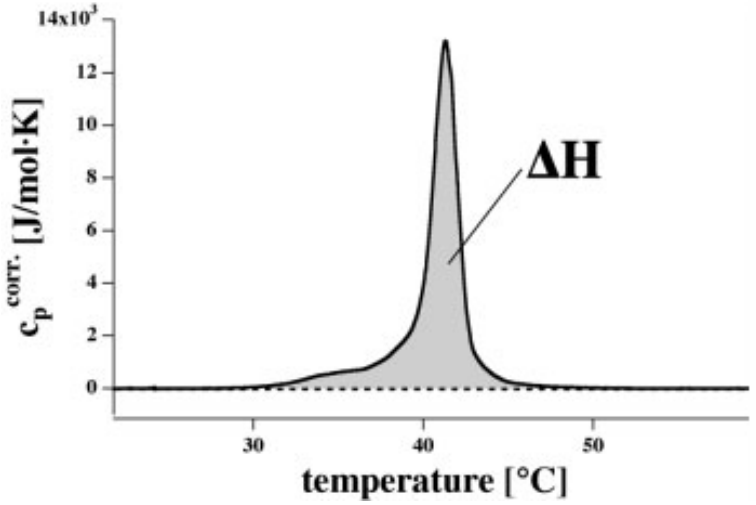

Figure 9: The phase transition profile of DPPC large unilamellar vesicles. The heat capacity C_p is measured in joules per mole per kelvin. The area under the curve determines the enthalpy in joule per mole. (Heimburg 2007)

In order to understand the effect of anaesthetics on the nervous system, it is necessary to have an understanding of properties of the membrane. The two models for nerve signal mechanism that we discuss in this thesis, both revolve around the plasma membrane, although they have opposing views on the roles of proteins and lipids. The Hodgkin-Huxley model gives proteins the main role of transporting ions over a passive lipid membrane, while in the soliton model, proteins attenuate the properties of the lipid bilayer which conducts a density pulse that is the nerve signal. Accordingly, the first model gave rise to a protein theory of anaesthetic mechanism, while the other revived the lipid

theory first proposed by Meyer and Overton giving it the mechanism that it originally lacked. Before we discuss these two models and their implications for anaesthesia, we give a brief introduction into nerve cells and the nerve signal.

2.4 Nerves and nerve signals

While understanding a phenomenon like consciousness still seems very far from our reach, the properties of nerve cells are quite possible to study in the lab, and have indeed been the subject of study ever since Galvani discovered the electrical stimulation of nerves in 1791.

Nerve cells, also called neurons, are similar to other cells in their basic molecular composition. They contain nuclei, mitochondria, endoplasmic reticula, Golgi apparatus, and all the other basic cell organelles, and they are separated from the environment by a plasma membrane. However neurons differ from other cells in that they are excitable, i.e. they are able to generate and conduct neuronal signals. This is a property they share with muscle cells.

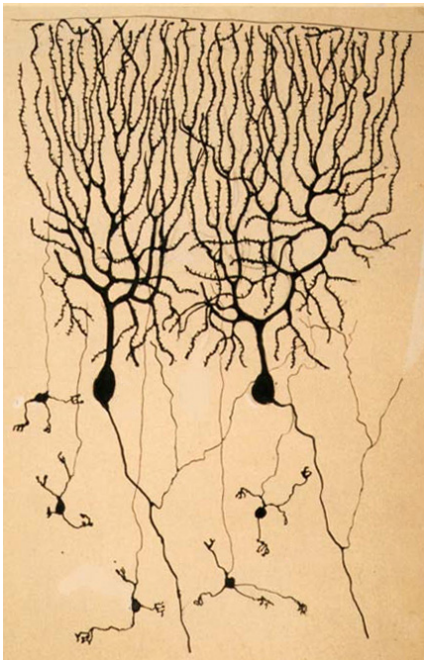

Figure 10: Drawings of neurons from pigeon cerebellum made by by Ramón y Cajal in 1899. (Wiki commons)

Before we delve into nerve signals, let us take a look at the structure of nerve cells. Nerves were first proposed to be independent cells connected to each other via synapses by pathologist Ramón y Cajal, who used the Golgi staining method (and improved on it) to study the nervous system. Neurons vary greatly in morphology, but they do share some basic features, which are shown in Figure 11. Most neurons are polarised, i.e. they have two different poles, a receptive and a transmitter. The cell body, also known as the soma, has many several processes emerging from it called dendrites, and together, the soma and the dendrites from the receptive pole of the neuron. Also emerging form the soma is the axon, which differs from the dendrites in its smooth appearance and uniform diameter. An axon may run for the length of up to 2 meters, while others are measured by the micrometer (Heimburg 2007). Before terminating, the axon divides into smaller branches in what is known as a terminal arborisation. Each branch contacts its target (usually another neuron or a muscle cell) via a synapse. The axon and its terminal arborisation form the cells transmitter pole. (Hammond 2015).

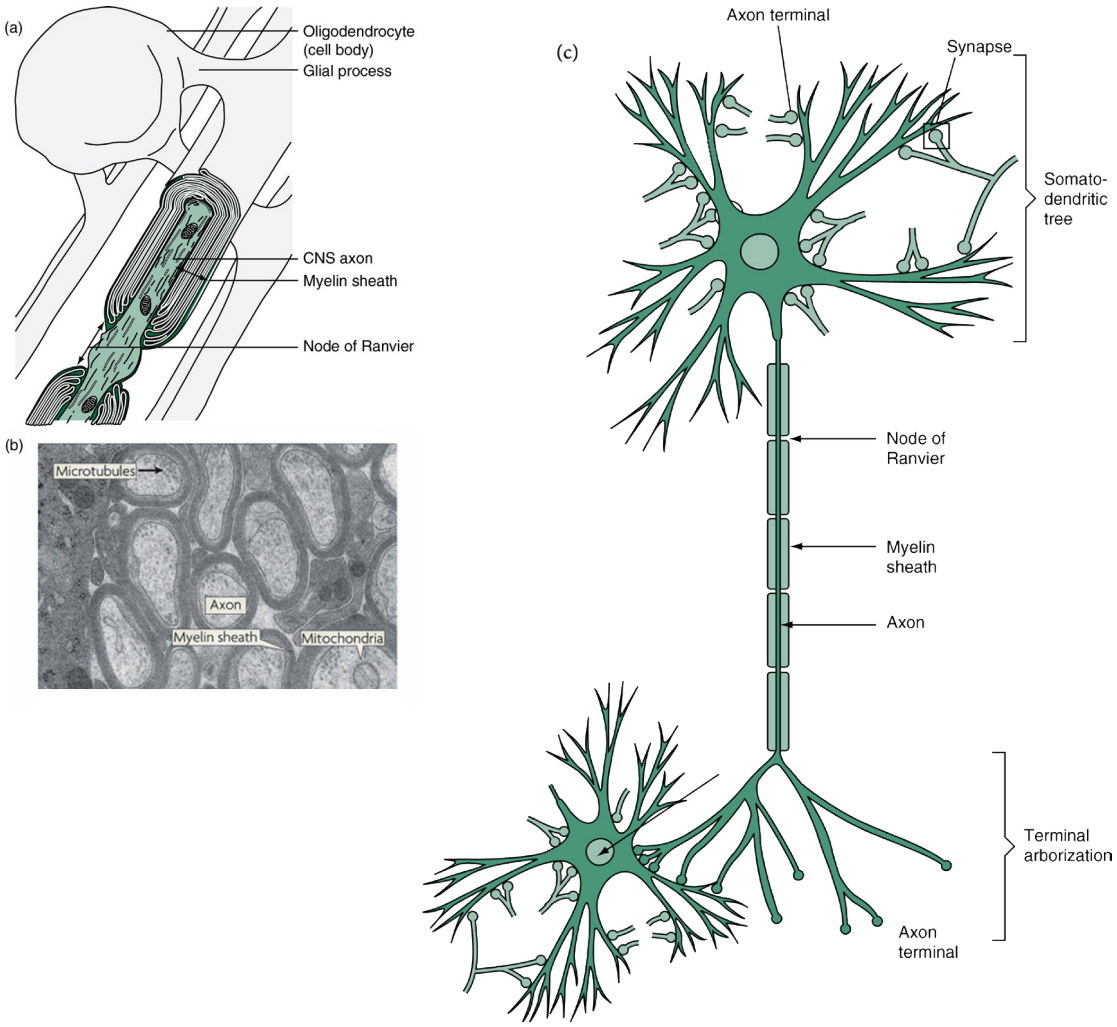

Figure 11:(a) A schematic drawing of the myelin sheath of an axon in the central nervous system formed by glial processes from oligodendrocytes. (b) Electron micrographs of a cross section myelinated axons in optic nerves. (c) A schematic drawing showing the basic structural features of neurons. (Hammond 2015)

Neurons are secretory cells, and their excretions are stored in the synapse and released in the synaptic cleft. The secreted molecules are known as neurotransmitters, as they are thought to facilitate the transmission of the signal from the neuron to its target.

The nervous system can be described as a network of neurons, each connected to many others via its receptive and transmitter poles. However, it does also contain several kinds of non-neuronal cells, collectively known as glial cells, which provide support and nutrition. Most notable are Schwan cells and oligodendrocytes, which extend their membranes into what is known as myelin sheaths, which wrap around nerve axons in compact spirals (see Figure 11). Myelination is found in vertebrate nerve fibers with a diameter greater than 1 µm. A prominent feature of myelination is that it occurs in long segments leaving gap between each segment and the next. These gaps are known as nodes of Ranvier. Myelinated nerves conduct impulses at a velocity of approximately 100 m/s, compared to a measly 1–5 m/s in nonmyelinated ones (Heimburg 2007).

This brings us to the nerve signal, which is classically defined as a transient change in

the membrane potential that propagates along an axon. This phenomenon is also known as the action potential. In all biological cells, there is an electric potential between the inside and outside. It varies between cell types, but it is always negative, inside relative to outside. In the squid giant axon, the resting membrane potential is -60 mV. The action potential starts with a rise in the membrane potential, which reaches its peak at +30 mV. This followed by a fall below the resting potential which reaches a nadir around -70 mV, before the membrane potential goes back to its resting value. (Keynes *et al.* 2011).

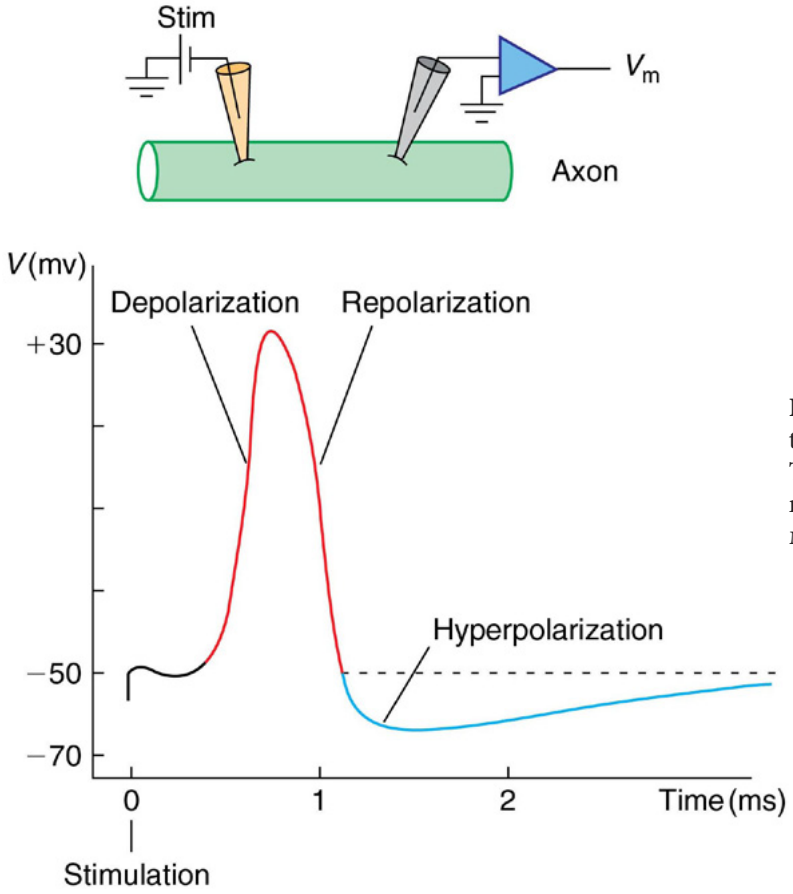

Figure 12: Action potential of the giant axon of the squid. The dotted line is the resting membrane potential (Hammond 2015).

The action potential is not the only component of the nerve impulse. It also has thermal, optical and mechanical components, which we will discuss later in this chapter. However, the electric component is the easiest to measure, and has therefore dominated scientific view of neuron activity.

2.5 The Hodgkin-Huxley model

The Hodking and Huxley model is a conductance based model, which is to say that it views the activity of the nerve as an ion current that passes through the membrane, which is modelled as the equivalent of an electrical circuit. The lipid membrane is con-

sidered to be a capacitor that also contains a resistor component which conducts an ionic current (Figure 13,a)

Hodgkin and Huxley developed their model based on voltage clamp experiments which they performed on giant squid axons. In voltage clamp experiments, two electrodes are inserted into the axon. The squid axon is usually used for these experiments because of its large diameter. One electrode measures the voltage, while the other injects a current necessary to keep the voltage constant across the membrane. The total current has two components, the capacitive current and the ionic one (Figure 13,b).

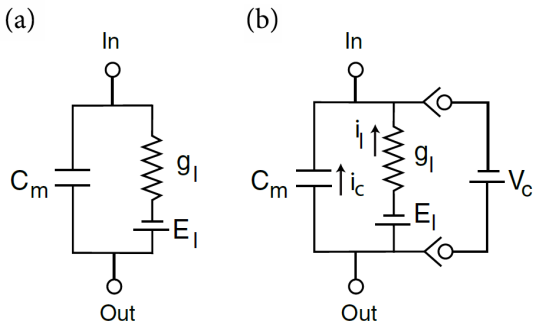

Figure 13: Equivalent circuit representation of the nerve cell membrane (A) In absence of voltage clamp. (B) With voltage clamp at constant voltage V_C. Cm: membrane capacitance; g_l: membrane leakage conductance; E_l: resting membrane potential; i_c = capacitative current; i_l = leakage current. (Edel 2015)

$$Total\ current = I_I + I_C$$

The capacitive current also contains two components:

$$I_C = C_m \cdot \frac{dV}{dt} + V \cdot \frac{dC_m}{dt}$$

The capacitance of the membrane is assumed to be constant, thus the second component is zero, and since the voltage is kept constant, the first component is also equal to zero. Consequently, the capacitive current is eliminated and only the ionic current remains.

By keeping the voltage constant over a time interval and measuring the current, H&H investigated the time dependence of the ion conductance, and by performing experiments using different voltages, they saw the voltage dependence of the ion conductance. Figure 14 shows the time dependence of the membrane current at 0 mV (solid trace).

The intracellular fluid in the giant squid axon contains a high concentration of potassium ions (400 mM), and a low concentration of sodium ions (50 mM). Conversely, the extracellular fluid has a low concentration of potassium (20 mM) and a high concentration of sodium (440 mM). H&H performed experiments where they exchanged the medium that surrounds the axon with one that does not contain sodium. In other experiments, they eliminated potassium ions from the internal medium. They interpreted the

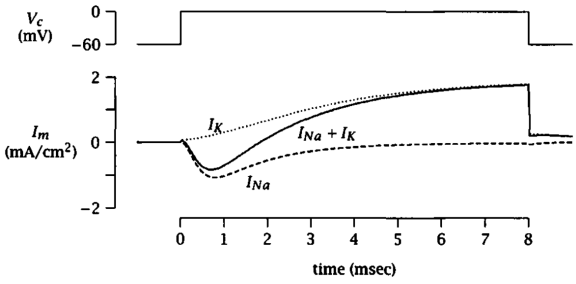

Figure 14: Voltage clamp measurement in giant squid axon (solid trace) in the absence of K or presence of TEA (dashed line) and in the absence of Na or presence of TTX (dotted line) (Johnston & Wu 1995).

remaining current in each experiment as resulting from the conductance of the ion that was not eliminated (Figure 14). A seperation of the two currents can also be obtained by applying tetrodotoxin (TTX) or tetraethylammonium (TEA) to the nerve, which are assumed to block the Na^+ and the K^+ conductance respectively. Based on these results, H&H concluded that the action potential is composed of an Na^+ current inwards and a K^+ current outwards.

The current of each ion can be calculated thus:

$$I_{Na}(V,t) = g_{Na}(V,t) \cdot (V - E_{Na})$$

$$I_K(V,t) = g_K(V,t) \cdot (V - E_K)$$

Where E is the Nernst potential for each ion, which depends on the concentration of the ion inside and outside the cell, and g is the conductance of the ion. Using this equation, H&H calculated the conductance of each ion by measuring I at a certain voltage V1, then after a second voltage pulse at a different voltage V_2. g does not have time to change between the two measurements.

The action potential can thus be described using this I-V equation:

$$I = C_m \frac{dV}{dt} + g_K(t,V) \cdot (V - E_K) + g_{Na}(t,V) \cdot (V - E_{Na}) + g_L(t,V) \cdot (V - E_L),$$

where g_L and E_L are the variables for a leak current through the membrane, which is mainly carried by $Ca^{++,}$ which in the squid axon has a higher concentration outside the cell than inside it by 4 to 14 fold. (Johnston & Wu 1995).

H&H found that the ion conductances do not follow simple equations, so they proposed used power functions to fit the data. To each gating particle, they assigned gating variables, which follow first order kinetics, thus each has a rate constant from closed to open and another from open to closed. These parameters are fitted from empirical data from the conductance measurements described above and cannot be measures independently. In the simplest form of the model, describing only two ion channels, these parameters add up to 12 (Heimburg 2007).

This local action potential, that results from the voltage and time dependent conductance of ions, is one of two basic elements of the Hodgkin Huxley model. The other is the passive diffusion of ions along the axon inside the cell and out. The nerve impulse can be described thus: The nerve signal starts with a local depolarization. The voltage sensitive Na^+ channels sense this change and opens as a result. They only do this if the voltage reaches a certain threshold. Na^+ ions travel down their gradient from outside of the cell towards the inside. This furthers the depolarisation across the membrane, which

the K^+ channels sense and open as a result. K^+ ions then travel through the channel across the membrane down their concentration gradient, thus restoring the membrane potential to its original value. When the voltage across the membrane changes locally, the area next to this local polarisation is still at the resting depolarized. Therefore, ions travel towards the depolarised area, thus producing a new local depolarisation which again starts a new action potential. To allow for a unidirectional travel of the impulse, the sodium channels are inactivated briefly following their activation. In the deactivation state, they cannot be opened by the depolarisation of the membrane.

In myelinated axons the majority of the axon surface is isolated by the myelin sheath, so that only nodes of navier can conduct ions. Thus the graded potential travels from one node to the next making the signal a much faster one.

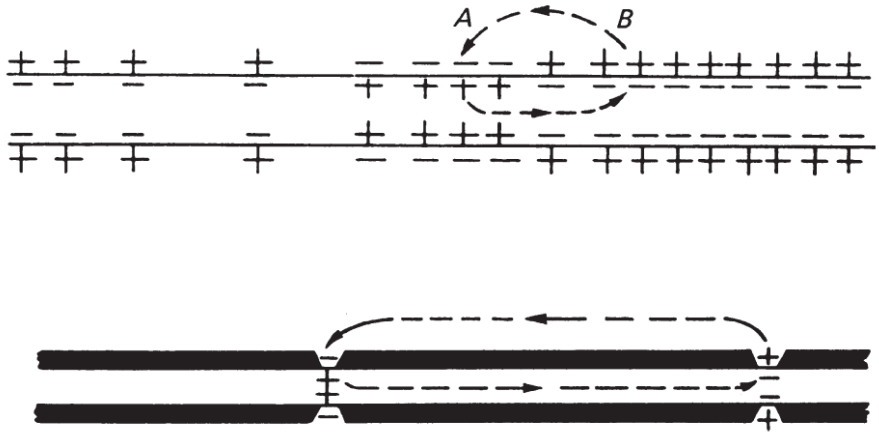

Figure 15: Propagation of the action potential through diffusion of ions. (Keynes *et al.* 2011)

2.6 Ion channels and the Protein theory of anaesthesia

When Hodgkin and Huxley proposed their model, they did not specify the ion conducting entities. It was however implied that the entities in question are protein ion channels. In 1976, the patch clamp, a technique developed by Neher and Sakmann, enabled electrical measurements over the cell membrane with minimal disruption. In this technique, a very small glass pipette is attached to the cell surface and suction is applied to ensure that the connection between the pipette and membrane is sealed (Figure 16, left). One electrode is inside the micropipette while the other is in the medium surround-

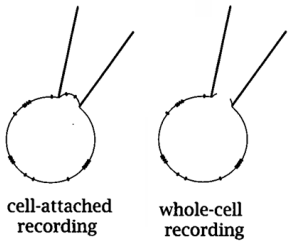

Figure 16: An illustration of the patch clamp technique (Johnston & Wu 1995).

ing the the cell. Like in the voltage clamp technique, the voltage is kept constant and a current is applied. By measuring the current, we measure the membrane permeability for ions. The membrane area that the pipette covers is small enough, that it is probable that only one protein ion channel is found in it. One can also make whole cell measurements by applying enough suction to rupture the patch of the membrane connected to the pipette (Figure 16, right).

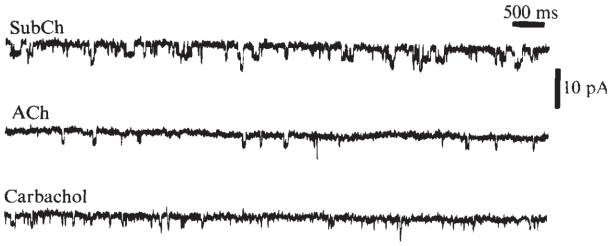

Figure 17: Patch clamp measurements of single-ion channel currents of different recepter ion-channels. Different cholinergic agonists were applied to the membrane to activate said channels (Neher & Sakmann 1976).

The patch measurements showed a stepwise increase and decrease in current. This was interpreted as single channel opening events, and it was seen as evidence of the existence of protein ion channels. This development had a huge impact on neuroscience, and opened up a new field of research: protein ion channels. Many different channels were identified and their properties studied. Such was the impact of this technique on medicine and physiology that Neher and Sakmann were awarded a Nobel Prize for "their discoveries concerning the function of single ion channels in cells" in 1991.

As protein ion channels were now seen as the main actor in nerve signals, they would logically be the first suspect in looking for an anaesthetic mechanism. However, classical ligand-protein binding requires specific interactions between certain amino acids in the protein's binding site and the ligand. Such specific binding is incompatible with the structural variety seen in anaesthetics. In 1984, Franks and Lieb provided evidence of anaesthetic interaction with proteins (Franks and Lieb 1985). In their article titled "Seeing the light", they used a firefly bioluminescent protein, luciferase, to show that anaesthetic potency is correlated to anaesthetic inhibition of proteins in a manner similar to the Meyer and Overton rule (Figure 18). The fact that Franks and Lieb used luciferase, a protein that is unrelated to the physiological function of nerves, illustrates the non-specificity of the protein-anaesthetic interaction. In a later paper, they conjecture that the binding sites are hydrophobic pockets in the proteins. Thus, they provide an explanation for the Meyer-Over-

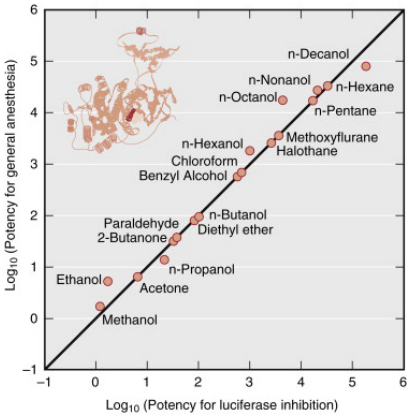

Figure 18: The correlation between anesthetic inhibition of luciferase and anesthetic potency. Miller 2005; adapted from Franks & Lieb 1994).

ton rule, while allowing for an explanation for the cut-off effect. This seems like a reasonable trade-off, however, molecule size alone cannot be the cause of the cut-off effect when some anaesthetic molecules are very large. Moreover, hydrophobic pockets are very common features (or defects) in proteins (Urban 2008), so why do not anaesthetics exert their effects on all cell proteins and inhibit all cell functions? Frank and Lieb suggest that the non-specific actions of anaesthetics seen in the lab become more specific at clinical concentrations.

Despite lack of evidence for such selectivity, a huge amount of research is allocated to studying ion-channel targets of anaesthesia. Textbooks list Gaba receptors, Acetylcholine and Glutamate Receptors, Ca^{++} channels and K^{+} channels among the many targets. (Miller 2005).

2.7 The soliton model

The scientific view on nerve activity remained overwhelmingly electricity centric for the last two centuries, and has very much remained that way till today, especially in the medical field. However, evidence has been accumulating over many decades that thermodynamic and mechanical changes occur in the neuron concurrently with the action potential, which the HH model could not explain.

A central figure in making and reporting these discoveries is biophysicist and physician Ichiji Tasaki, who is most known for discovering the isolating properties of the myelin sheath; a discovery that contributed to the current scientific view of nerve imulse propagation. Tasaki and collaborators found that the fluorescence intensity of lipid dyes, which they found to change during in the squid giant axon as well as the crab leg nerve. This was accompanied with an increse in the fluorescent anisotropy, indicating a decrease in the rotational mobility of the dyes (Tasaki *et al.* 1969).

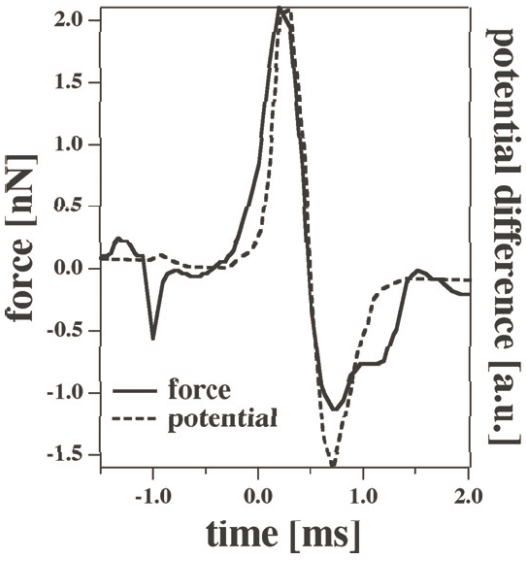

Figure 19: Force on a piston (dotted curve) during the action potential in a squid axon (solid line is the voltage change). (Heimburg & Jackson 2007. Adapted from Iwasa & Tasaki 1980).

By measuring the force exerted by the nerve surface on a piston, Tasaki and co. found that the nerve thickness changes with about 1 nm concurrently with the action potential (Iwasa *et al.* 1980).

The finding that clashes most clearly

with the HH model is the reversible heat change which occurs during the action potential. Heat release during the action potential was first described in the 1920's by A. V. Hill. In 1958, Abbott, Hill and Howarth found that the initial heat release which is then compensated for almost completely by a heat absorption as seen in Figure 20 (Abbott *et al.* 1958). In myelinated nerves, the heat change seemed to originate from the whole nerve rather than only from the nodes of Ranvier, which indicated that the heat release in is not related to ion currents. The two phase nature of the change is detrimental, because the ion conduction in the HH model would be an exothermic process.

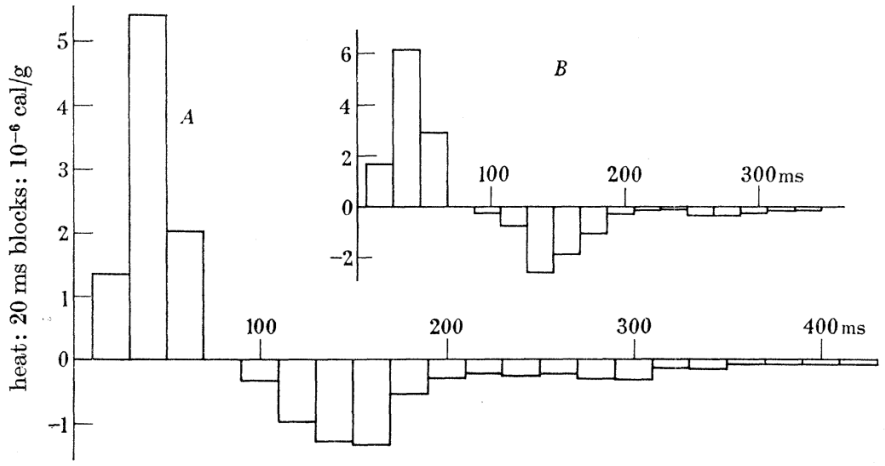

Figure 20: Heat release and absorption due to a single stimulus at 0 °C. Each block represents 20 ms. **A** is a mean of five experiments and **B** shows recording from a single experiment (Abotth *et al.* 1958).

In 2005, Thomas Heimburg and Andrew Jackson observed that, the biological membrane in physiological temperature is always on the brink of its phase transition. They found this to be true in two bacteria species E. Coli and B. Subtilis (Heimburg & Jackson 2005). Later, the same observation was made in rat brain (Madsen 2012). In this project we investigate sheep spinal cord, and our results agreed with the previous observations.

The changes that occur in the nerve during the impulse described above correspond to the changes that occur in the lipid phase transition; the thickness change, the area change of the lipid bilayer with the change in length of the nerve, and the change in rotational freedom. This leaves the most prominent aspect of the impulse; the voltage change. How can it be related to a phase transition? The answer lies in the membrane capacity, which H&H assumed to be constant. When the thickness and area of the bilayer change, the capacitance changes accordingly (Heimburg 2007).

$$C_m \propto \frac{A}{d}$$

When lipids transition from the gel phase to the liquid phase, its area increases while its thickness decreases resulting in a change in the capacitance.

Considering this in addition to the adiabatic nature of the nerve impulse, Heimburg and Jackson were led to compare it with a process that is also mechanical and adiabatic; the sound wave. They proposed that the nerve impulse is a form of density wave, akin to sound waves. This wave can be described as a soliton, a self-sustaining solitary wave that maintains its shape and does not attenuate while propagating. For a soliton to exist, there are two requirements. The first is non-linear elastic constants. The elastic constants of the membrane are unchanging except during the phase transition. Heimburg & Jackson showed that during the phase transition, the compressibility and heat capacity are closely related as shown in Figure 22, right. The other requirement is the frequency dependence of sound velocity. Here also, Heimburg & Jackson showed that the adiabatic area compressibility of lipids is a decreasing function of frequency, which means that higher frequency results in higher propagation velocity as shown in Figure 22, left

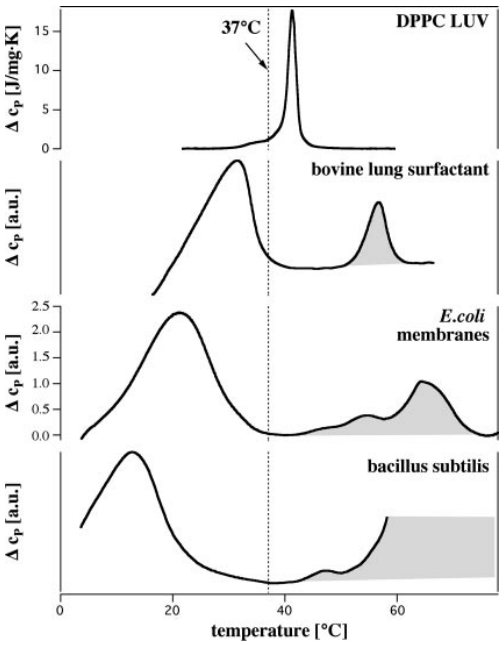

Figure 21: The heat capacity profiles of DPPC vesicle, bovine lung surfactant, and two bacteria membranes. For the biological samples, the peaks prior to the physiological temperature shows reversibility and is therefore attributed to lipids. The peaks highlighted in grey is irriversible and is therefore attributed to protein unfolding (Heimburg & Jackson 2005).

Another important finding about lipid membranes during the phase transition is that they form ion channels. When patch clamp measurements are preformed on lipid membranes in the absence of proteins, the same channel-like opening events that have been attributed to proteins are seen (Wodzinska *et al.* 2009; Gallaher *et al.* 2010). This finding puts the validity of patch-clamps

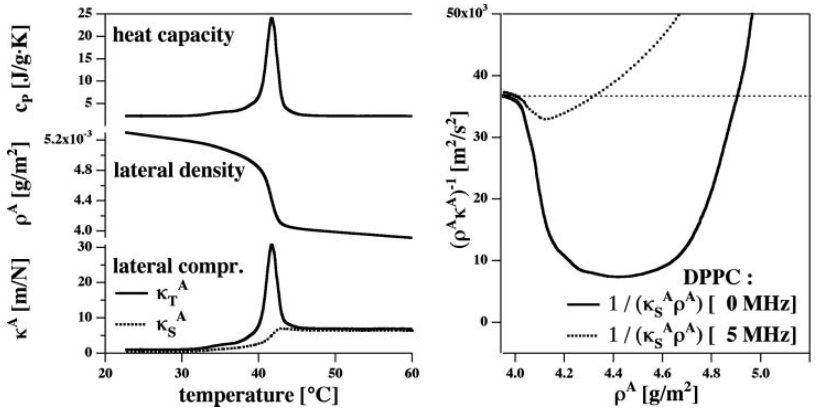

Figure 22: Lipids membranes fulfill the soliton requirements during the phase transition. Left: Heat capacity of DPPC large unilamellar vesicle (Top), lateral area density, A (Middle), and the corresponding lateral compressibility (Bottom). Right: The lateral sound velocity for the low-frequency and the 5-MHz case, as a function of membrane area density at T 45 °C (Heimburg & Jackson 2005).

studies on proteins into question.

The soliton model has great implications for anaesthesia research as it provides us with a mechanism that is compatible with the Meyer-Overton correlation.

2.8 Melting point depression

We come back to the Meyer Overton hypothesis of anesthesia mechanism, which proposed that anesthetics act by adsorbing into lipids and changing their physical state. The hypothesis did not specify what physical state is being changed and how it affects nerve action. In the latter half of last century, several studies showed that general and local anaesthetics lower the melting temperature of lipids (Engelke *et al.* 1997; Hata *et al.* 2000; Græsbøll *et al.* 2014).

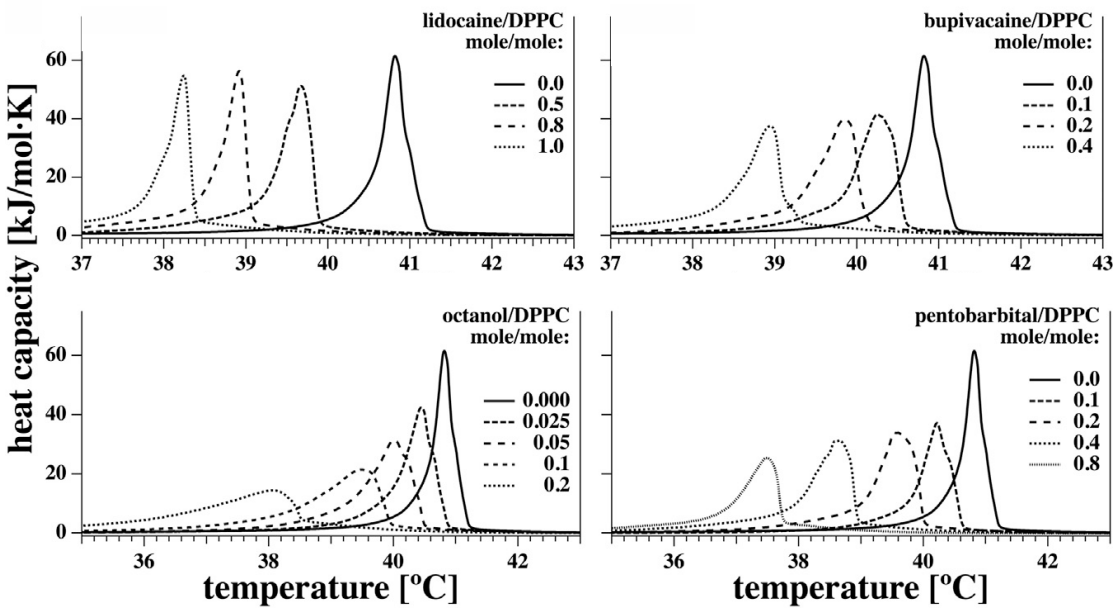

Figure 23: The effect of general anaesthetics (octanol and pentobarbitallocal anaesthetics (lidocaine and bupivacaine) on the phase transition of 10 mM DPPC LUVs. The amount of anawesthetic is given as a mole ration relative to DPPC. (Græsbøll *et al.* 2014)

The theoretical explanation for this effect is akin to the effect that salt imposes on the melting temperature of ice. The solute is soluble in the fluid phase and insoluble in the solid/gel one; therefore it is more energetically favourable for the whole system for the solvent to exist in the fluid phase. According to the Freezing-point depression law,

$$\Delta T_m = \frac{-R \cdot T_m^{\,2}}{\Delta H} x_A$$

the change in melting temperature T_m is directly related to the molar fraction of anaesthetic in the membrane x_A for low solute concentrations and assuming perfect misci-

bility in the liquid phase and immiscibility in the gel phase. (Heimburg & Jackson 2007). R is the gas constant and ΔH is the enthalpy of the transition.

This effect provided a possible answer for the cut-off effect, as the longer alcohol were shown to either have no effect on the melting temperature of lipids or raise it (Figure 24) (Kaminoh *et al.* 1992). However, it was still unclear how the depression of the melting temperature would affect nerve function.

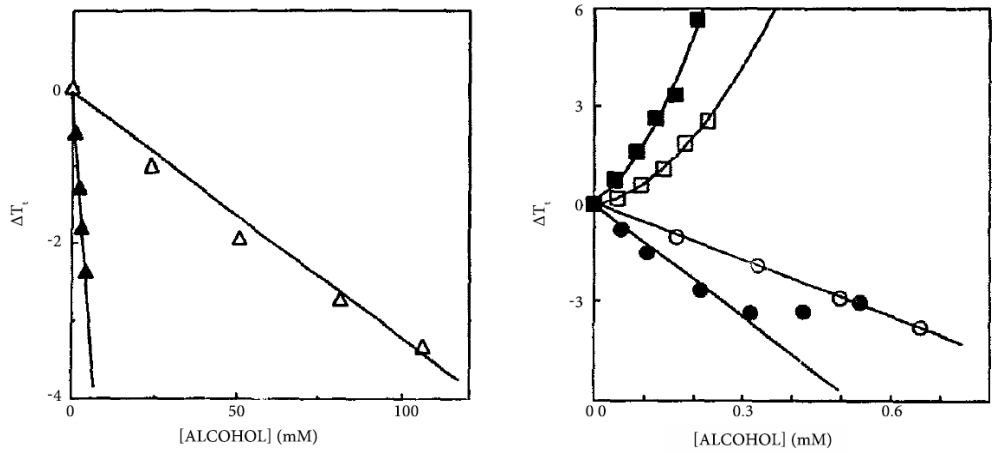

Figure 24: Effect of n-alcohols on melting temperature of 1 mM DPPC vesicles. 1-butanol (empty triangles), 1-hexanol (solid triangles), 1-octanol (empty circles), 1-decanol (solid circles), 1-tridecanol (empty squares), and 1-tetradecanol (solid squares) (Kaminoh et al. 1992)

Another previously impenetrable anaesthesia-related phenomenon that becomes easily explainable is the pressure reversal of anaesthesia. It has long been known that pressure reverses the effect of anaesthesia. This effect was first noticed in tadpoles and later also shown in Newts and mice (Lever *et al.* 1971; Miller 1977). The effect of pressure on the lipid phase transition is opposite that of anaesthesia, as it raises the melting temperature. This effect is related to the effect of pressure on specific volume of the lipid membrane upon melting:

$$\Delta T_m = \frac{\Delta p \cdot \Delta V}{\Delta H} \cdot T_m$$

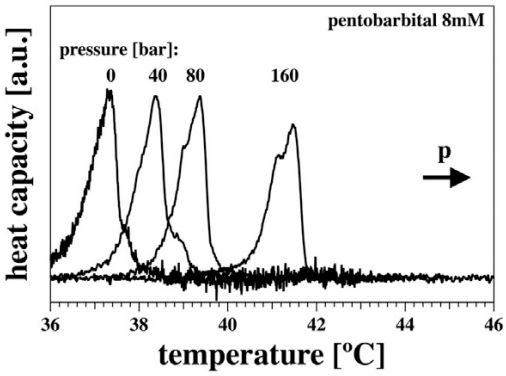

Figure 25: The effect of pressure on the phase transition of 10 mM DPPC LUVs in the presence of 8mM pentobarbital. The same effect was also shown in the presence of local anaesthetics lidocaine and bupivacaine (data unshown) (Græsbøl *et al.* 2014).

As seen in Figure 25 pressure also exerts this effect in the presence of anaesthesia, thus reversing the effect of the anaesthetic on the melting temperature (Græsbøl *et al.* 2014)

With the emergence of the soliton model, the link between the phase transition and nerve function has become clear. When the melting temperature is shifted downwards,

the biological membrane at a physiological temperature becomes further away from the phase transition and a larger stimulus is needed to induce a nerve impulse. The soliton model predicts that anaesthetics do not block the nerve signal. Instead, they change the stimulus response relationship. A study done on frog nerves showed that the general anaesthetic xenon and local anaesthetic procaine do indeed shift stimulus response curve (Figure 30).

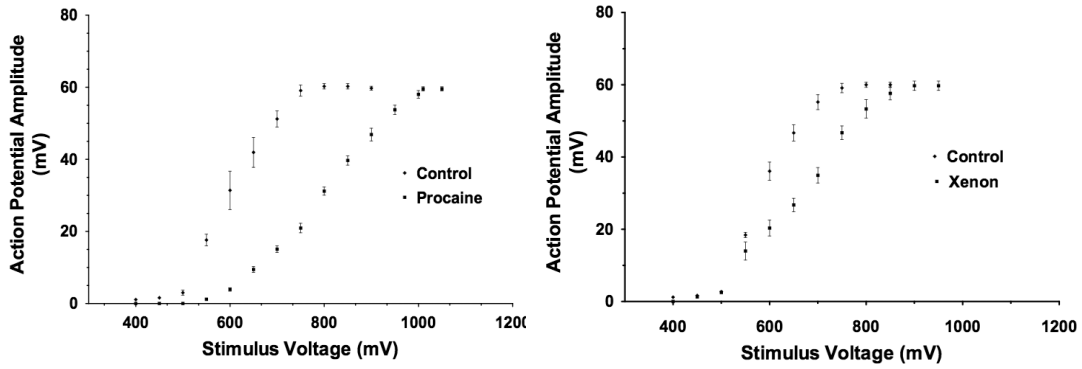

Figure 30: The amplitude of the action potential as a function of the stimulus voltage in the presence and absence of local anaesthetic procaine (left) and general anaesthetic xenon (right) (Khassahun et al. 2010).

In the next chapter we will investigate whether the effect of the alkane on the phase transition of lipids can explain the cut-off effect in accordance with the soliton model.

CHAPTER 3

THE CUT-OFF EFFECT IN ALKANES

In this chapter, we investigate the effect of n-alkanes: n-hexane, n-octane, n-nonane, n-decane, and n-dodecane on the phase transition of DMPC (1,2-dimyristoyl-sn-glycero-3-phosphocholine) large unilamellar versicles (LUVs). We chose DMPC because it is a common lipid in biological membranes. When hydrated, lipids form multilamellar vesicles (MLVs) onion-like structures with many bilayers on top of each other. We get ULVs by extruding the sample as we will describe below. We use a DSC to record the heat capacity profile over temperature of the sample.

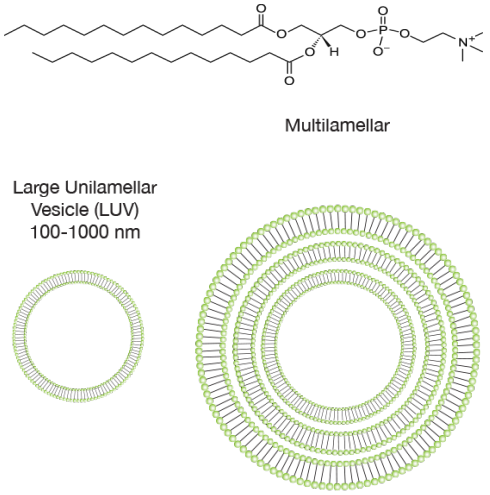

Figure 26: Chemical structure of DMPC (Top)and a shecmatic drawing of MLV and ULV structure (bottom).

3.1 The differential scanning calorimeter (DSC)

In this project, we used the VP-DSC from Microcal.

The DSC has two cells, a sample cell and a reference cell, which are heated (or cooled) at the same rate. The two cells are heated individually, and the temperature of each is

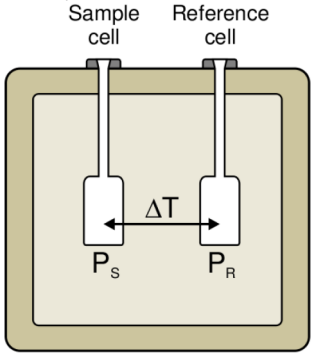

measured.

When a difference in temperature between the two cells occurs, a feedback loop ensures that the power with which the sample is heated is changed in order to compensate for this difference. The apparatus measures the power with which each cell is heated. The difference between the two powers is integrated over a time interval which gives us the heat added.

$$\Delta Q \simeq \Delta P \cdot \Delta t$$

The heat capacity can then be calculated by dividing the heat added over the heating rate.

$$C_p = \frac{\Delta Q}{\frac{\Delta T}{t}}$$

3.2 Preparing the samples

DMPC was purchased from Avanti lipids. It was stored in the freezer at -15 °C at all times except for when it was being used. The bottle was taken out of the freezer and allowed to thaw in the unopened container until it reached room temperature. This is done so as to prevent prevents the lipids from absorbing water from the surroundings.

We started by preparing a stock solution of DPPC in chloroform, which allowed us to measure equal amount of lipids in our samples. The chloroform was then dried off under an air stream, then the samples were put in a vacuum chamber for 3-5 hours to ensure that all the chloroform has evaporated.

Then buffer was added to each sample for a lipid concentration of 10 mM. The buffer we used contained 1mM Hepes, 1mM EDTA and 150 mM KCl and was adjusted for pH = 7.42 using KOH and HCl. Hepes is a pH buffer, and EDTA binds Ca^{++} thus inhibiting bacteria growth.

The sample was briefly put under a stream of hot water to help the lipids dissolve in the water, then it was vortexed until all lipids dissolved and. At this point, we would have multilamellar vesicles (MLVs). To get ULVs we extruded the using a Mini-Extruder from Avanti Lipids. In the extrusion process, the sample is passed from one syinge to another and back through a porous polycarbonate membrane at a temperature above the lipid's melting temperature. We used a membrane a pore size of 100 nm. The sample was passed through the membrane 15 times at 40 °C The extrusion process was automated and the speed was constant at 1.4 minute per pass. According to the manufacturer, a minimum of 11 passes through the membrane is required to completely shift the vesicle size distribution.

Each sample was degassed for 10 minutes along with the buffer, before adding it to the calorimeter cells in order to remove air bubbles.

The shortest alkane we tested, hexane, is volatile, therefore we added the alkanes to the sample after extrusion and degassing. Because of the small volume needed, we added the alkanes dissolved in methanol. Since methanol effect the lipid phase transition, we started each series with a pure lipids sample, then a sample to which we added methanol without any alkane. All alkanes were added in the same way in order for our experiments to be comparable. To add different amount of the alkane to the samples we prepared different concentrations of alkane in methanol so as to keep the amount of methanol added to the sample constant in the series. Methanol concentration was 0.25 M in all samples. Its affect on the melting temperature is small despite the high concentration because of its low partition coefficient. Hexane and octane were added to the sample at 4 °C to avoid evaporation. Temperature appropriate densities were calculated using data from Yaws' Thermophysical Properties of Chemicals and Hydrocarbons (Yaws 2014).

The only exception to this was dodecane, which was not soluble in methanol at room temperature. It is soluble in ethanol, but we opted for adding it to the sample directly without any solvents. It was added after extrusion and degassing.

For the longer alkanes, nonane, decane and dodecane, we compared the sample to an equal volume of buffer to which we added the same amount of alkane. We observed that the dodecane formed droplets on the surface of the buffer despite continuous mixing, but no droplets were visible on the lipid sample. Therefore, we concluded that dodecane did dissolve in the lipid sample. It should be noted, that the volume was very small and the transferpettor we used was not precise at that small volume ranger, therefore the concentration of dodecane in the sample has a large margin of error.

All transferring of chloroform, methanol or alkanes was done using either a glass syringe or a transferpettor with a glass tip.

All containers and equipment were cleaned with water and ethanol and dried with nitrogen or an air stream before use.

3.3 Using the calorimeter

The sample was added to the calorimeter using a glass syringe with a long tip. We started by adding the buffer into the reference cell. The syringe tip is inserted into the cell the liquid is added until it overflows into the reservoir. The excess is then removed using the syringe.

Each sample was scanned 4 times in the 5 °C to 45°c interval in alternating up- and downscans. The first two scans were at 40 deg/h, and where not used in the results. The second two scans were done at 5 °C/h. These are the scans represented in the result section. The up- and down scans are not identical because of hysteresis. To eliminate the difference between the two, we would have to go to very low scanning rates, which would be time consuming.

After each experiment, the calorimeter cells were cleaned using the cleaning devise provided by the manufacturer. The devise had a long needle that is inserted into the cell to be cleaned and a long narrow tube which is inserted into the cleaning solution. It would continually pump the solution into the cell and out into a waste container.

The cells were cleaned thus:

Reference cell:	Ethanol	5 min
	Water	10 min
Sample cell:	Ethanol	10 min
	Water	15 min

The syringe was cleaned thoroughly with ethanol then water, then dried with nitrogen.

3.4 Data analysis

Data obtained from DSC scans was analysed on Igor Pro 6.37 using modules written by Thomas Heimberg and Kaare Græsbøl. The modules find the base line of the data after manual selection of the phase transition area. The baseline was always fitten with a 5th degree polynomial. After substraction of the baseline fit, the module located the peak melting temperature (T_m), the upper phase boundary (UPB) and the half-enthalpy temperature.

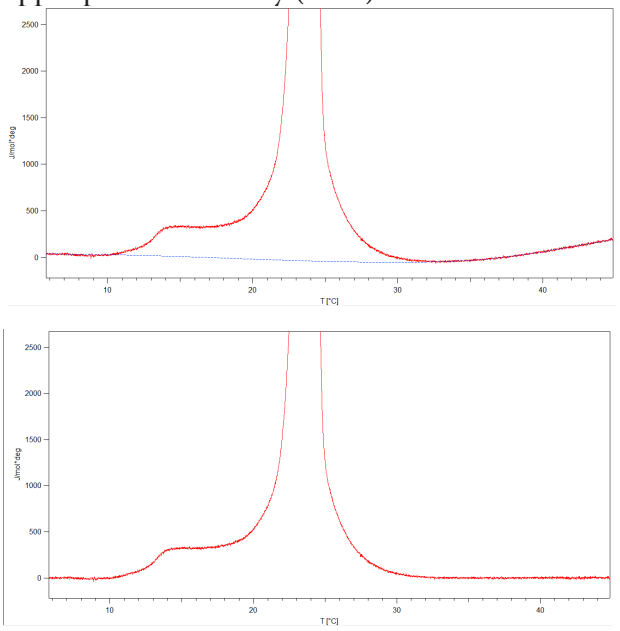

Figure 31: Top: A DSC scan of a DMPC 10mM ULV sample before baseline sbstraction with fitted basline (blue trace). Bottm: Same scan after substracting the fitted baseline.

3.5 Results

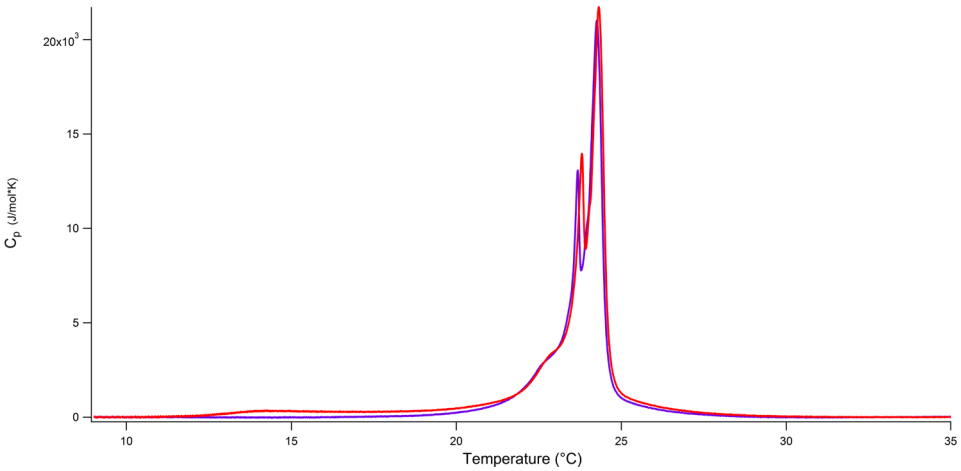

Figure 32: Excess heat capacity of the phase transition of DMPC LUVs. Upscan (red) and downscan (blue) of the same sample

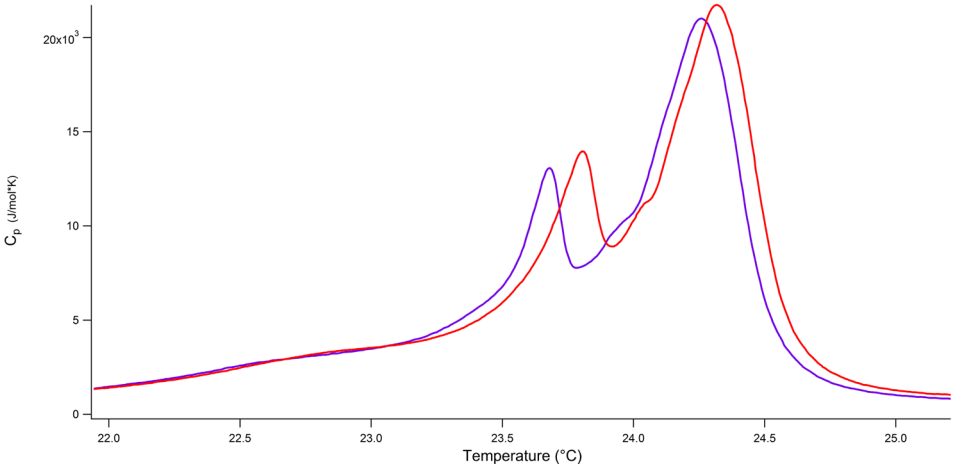

Figure 33: Excess heat capacity of DMPC LUVs. Upscan (red) and downscan (blue) of the same sample. Same scans as in Figure 33

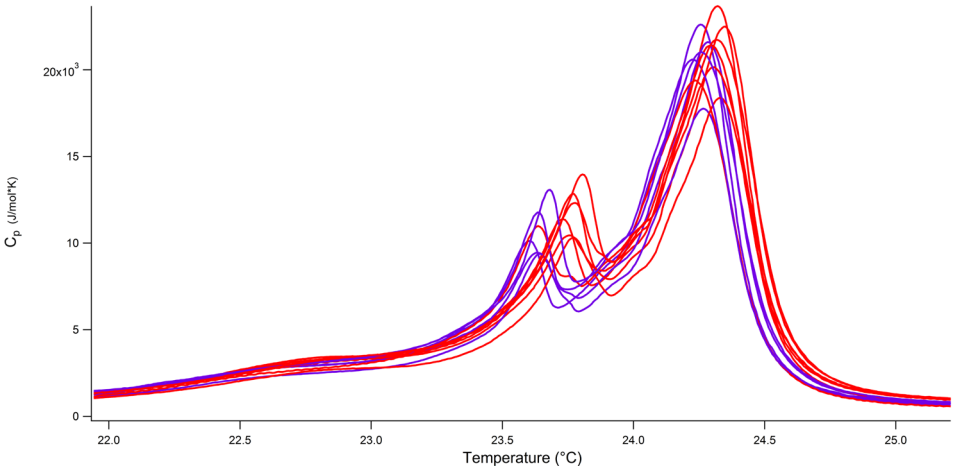

Figure 34: Excess heat capacity profiles of several different DMPC LUV samples. One upscans (red) and one downscans (blue) from each sample.

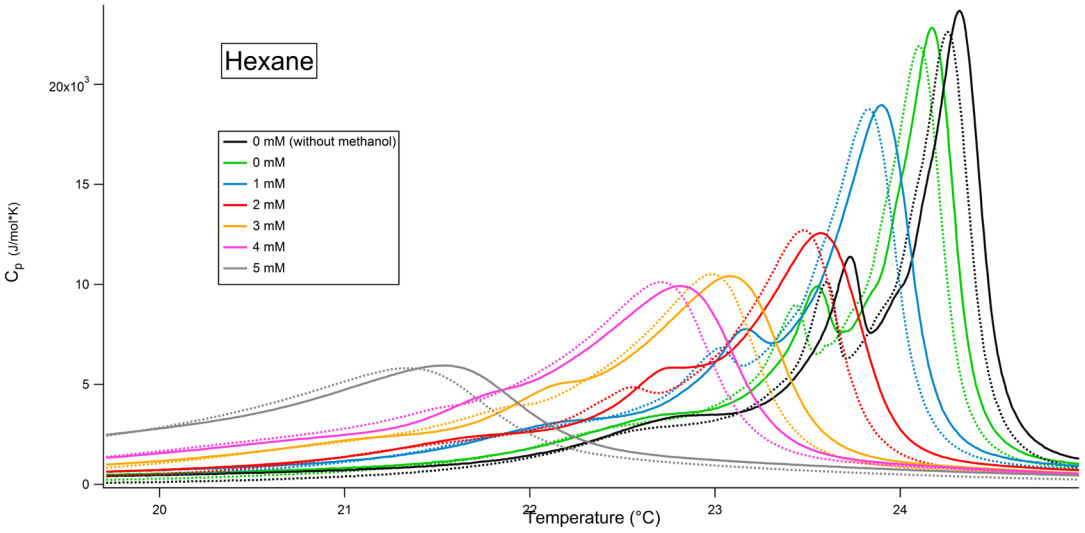

Figure 35: Heat capacity profile of 10 mM DMPC LUV with different concentrations of n-hexane. All sample but the first in the series contain 0.25 M methanol.

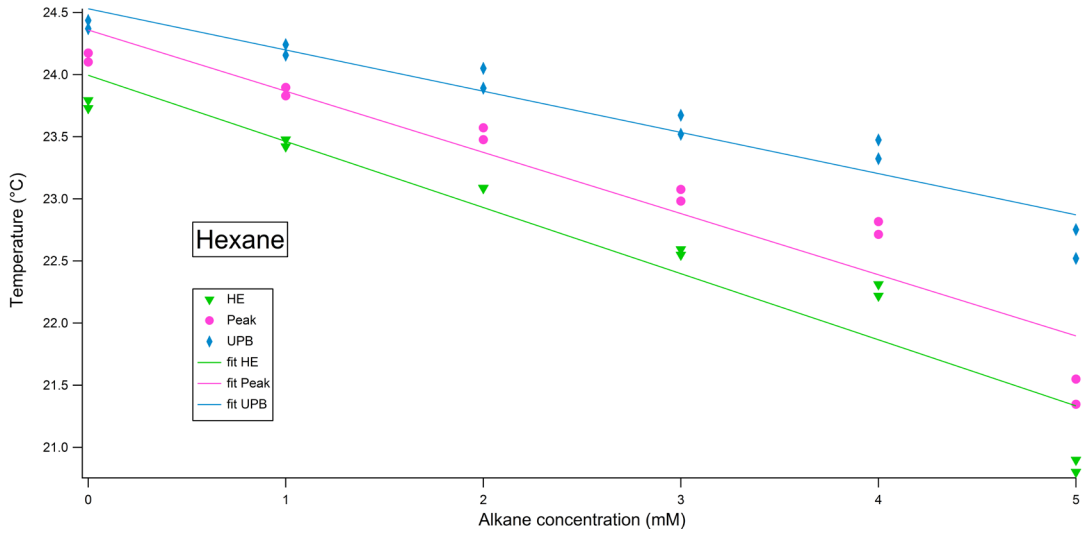

Figure 36: The peak temperatures (T_m)., half enthanlpy temperatures, and upper phase boundary temperatures calculated from the profile in Figure 35 (excluding the sample without methanol)

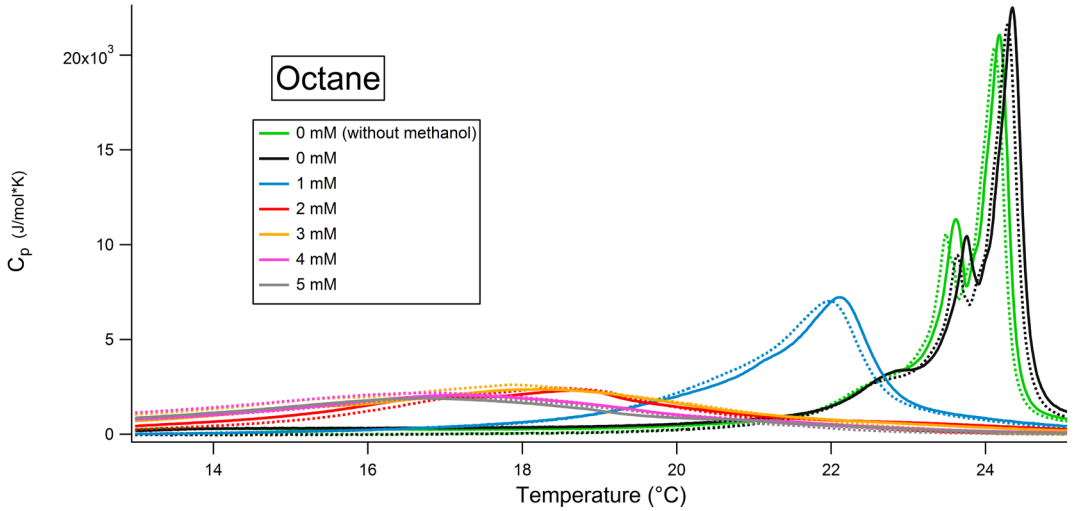

Figure 37: Heat capacity profile of 10 mM DMPC LUV with different concentrations of n-octane. All sample but the first in the series contain 0.25 M methanol.

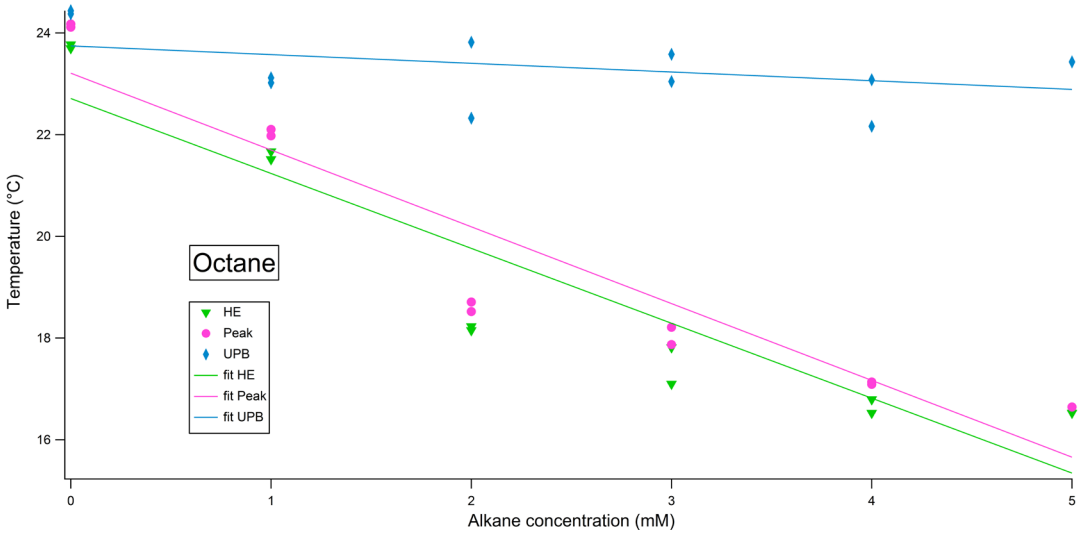

Figure 38: The peak temperatures (T_m)., half enthanlpy temperatures, and upper phase boundary temperatures calculated from the profile in Figure 37 (excluding the sample without methanol)

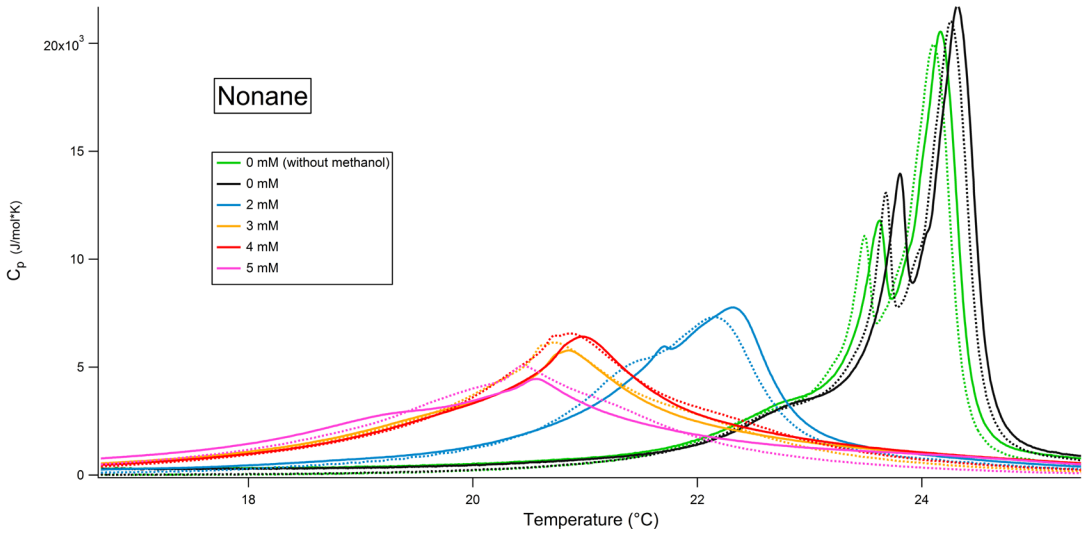

Figure 40: Heat capacity profile of 10 mM DMPC LUV with different concentrations of n-nonane. All sample but the first in the series contain 0.25 M methanol.

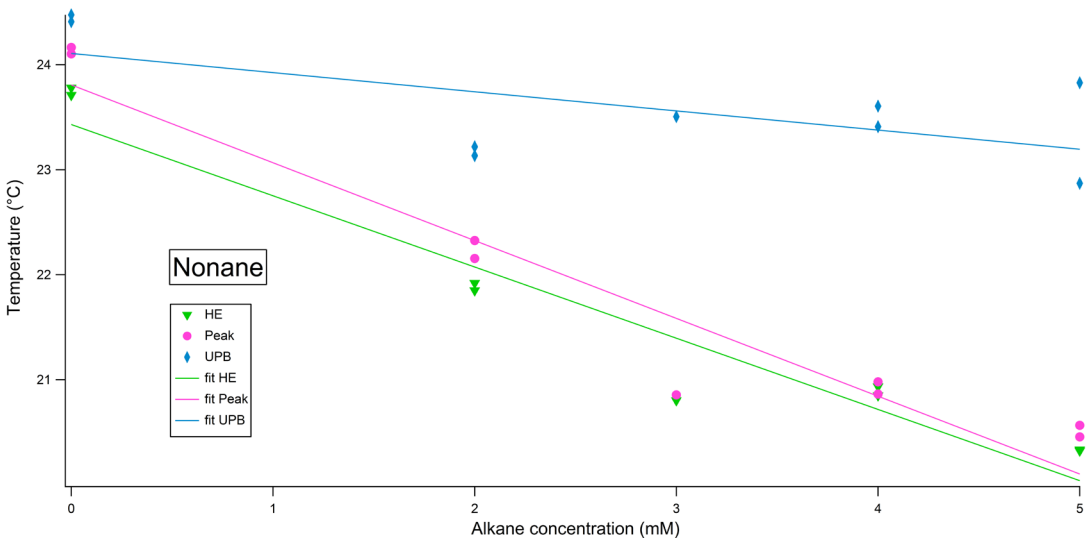

Figure 41: The peak temperatures (T_m)., half enthanlpy temperatures, and upper phase boundary tempertaures calculated from the profile in Figure 40 (excluding the sample without methanol)

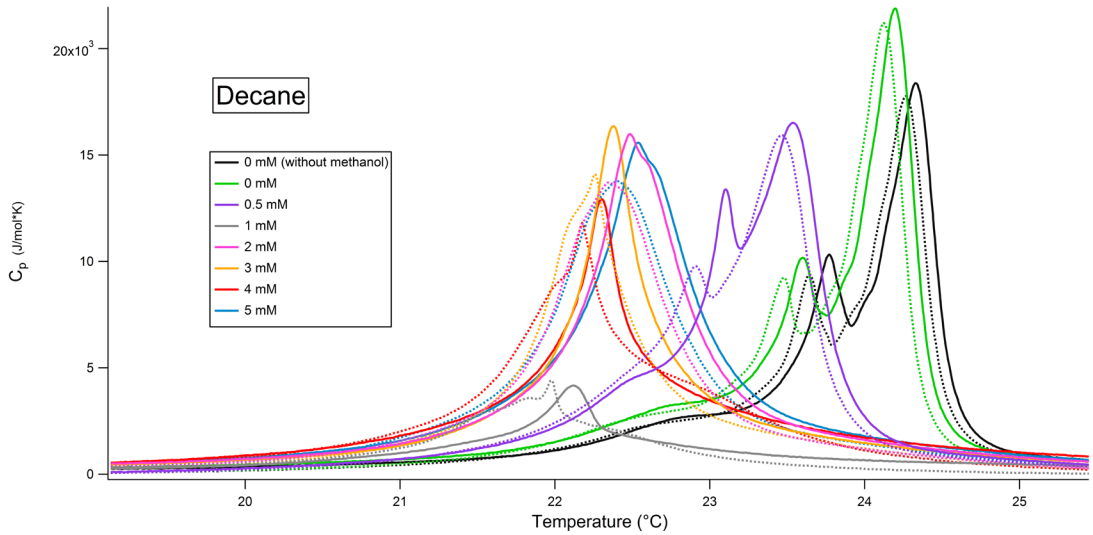

Figure 42: Heat capacity profile of 10 mM DMPC LUV with different concentrations of n-decane. All sample but the first in the series contain 0.25 M methanol.

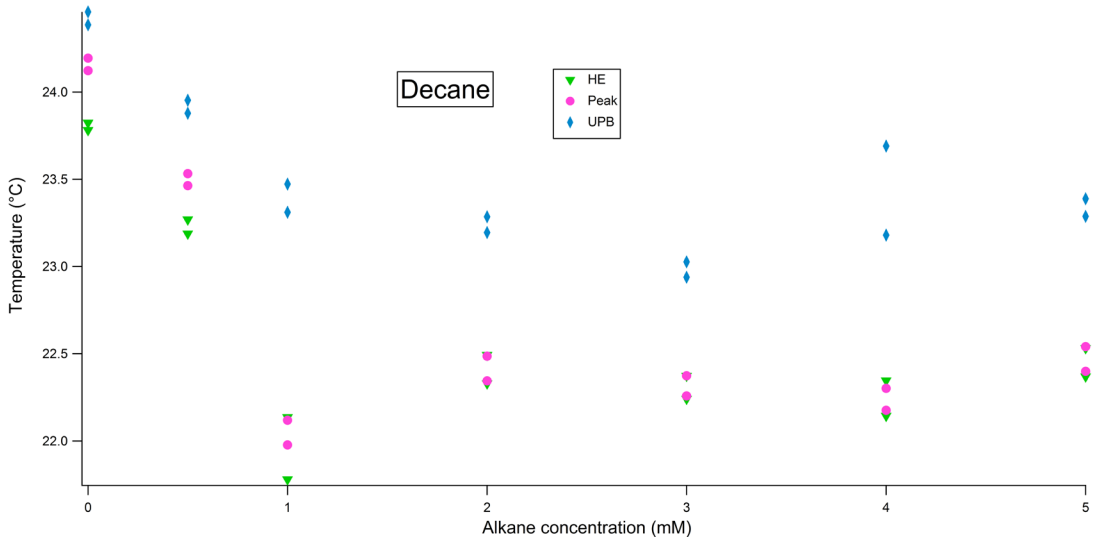

Figure 43: The peak temperatures (T_m)., half enthanlpy temperatures, and upper phase boundary temperatures calculated from the profile in Figure 42 (excluding the sample without methanol)

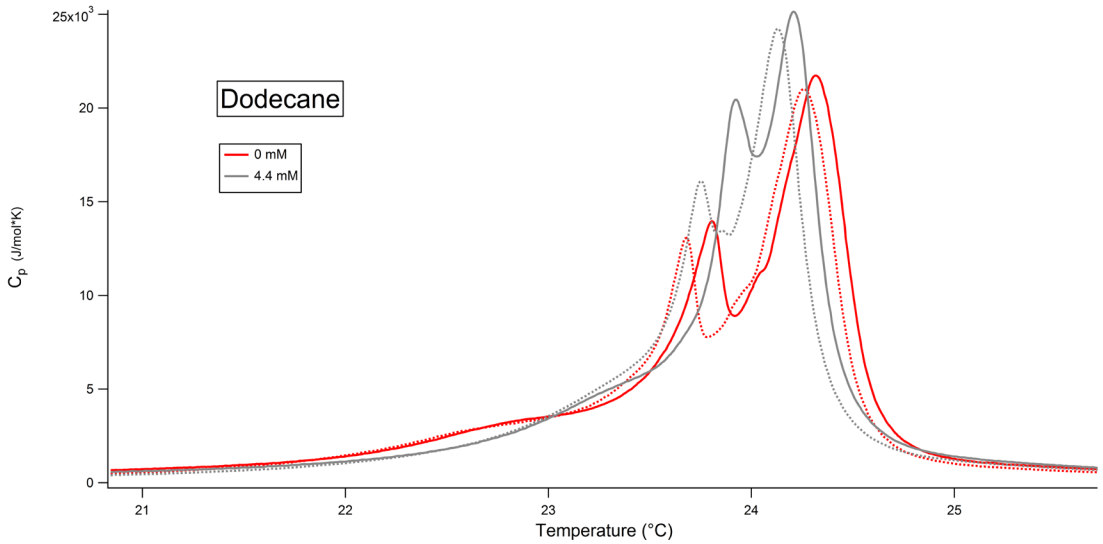

Figure 44: Heat capacity profile of a 10 mM DMPC LUV with or without n-dodecane.

3.6 Discussion

The phase transition of DMPC starts at around 12 - 13 °C with a pre transition ramp. This pre transition is almost completely flattened out in downscans but is definitely present in upscans. Then comes the main phase transition between around 22 and 25 °C. There are two peak, a smaller one a little above 23.5 °C, then a larger one alittle before 24.5 °C. There is very little variation in te peak temperature between the different DMPC samples, but there is a somewhat significant difference between downscans and upscans, which is due to hysteresis, i.e. the state of the system is affected by its history.

In the hexane series we see a very regular decrease in the melting temperature of DMPC. The change in the shape of the profile seems systematic. The peak temperature, half enthalpy temperature (the temperature at which half the total transition enthalpy has been absorbed/released) and the upper phase boundary all follow linear regressions with not too dissiular slopes.

In the octane series the change in the phase transition shape and peak temperature is very dramatic and seems to reach a point of saturation between 4 mM and 5 mM octane. Tm, and HE do not follow the linear regression as nicely as in the hexane series . The change in the upper phase boundary is much smaller than in hexane.

The irregularity continues witn nonane which already seems to reach a point of saturation between 3 mM and 4 mM. Here again, Tm and HE decrease but deviate from linearlity. The change in UPB is also small here.

in the decane series the change in the phase transition seems somewhat rampant. There is not regular tendency towrds bradening out the profile. The 1 mM concetration has the lowest peak temperature and the heat capacity profile for this sample is very flat. Tm, HE and UPB do not seem to follow a linear regression.

We arrive finally at dodecane, which does not seem to have an effect on the melting temperture, and rather than broadening the heat capacity profile, it makes it narrower

The slopes of the fitted linear regressions are as flows:

	Slope (T_m)	Slope (HE)	Slope (UPB)
Hexane	-0.49247	-0.5322	-0.33173
Octane	-1.5103	-1.4736	-0.17083
Nonane	-0.74113	-0.67846	-0.18247

The decrease of Tm and HE is higest at octane, while the decrease of UPB is highest at hexane.

Our results are generally in accordance with the cut-off point in anesthetic potency for alkanes. Hexane, octane and nonane whose anesthetic potency corresponds to they partition coefficient all decreased the melting temperature. of the lipid. Decane also

dcreased the melting temperature, but not in a progressive concentration dependent manner. Dodecane had very little effect of the melting temperature despite the high concentration.

In these experiments, we used the same concentrations for all the alkanes, however it might have been a better idea to start out with smaller concentrations for octane and nonane which have higher partition coefficients than hexane. At the higer concentrations, the effect of the two alkanes seemed to reach a kind of plateau.

We now move from a solved mystery to an unsolved one.

CHAPTER 4

EPILEPSY: THE OTHER SIDE OF THE COIN?

When explaining epilepsy in layman terms, medical practitioners often grab for the expression "electrical storm in the brain". This of course reflects the electricity centric view on nerve function based on the HH model. The academic definition of an epileptic seizure is "hyper-synchronous firing of a large number of cortical neurons" (Perks 2012).

The stereotypical picture of an epileptic seizure is of a person lying on the ground with stiffened limbs and convulsing movements (Figure 27). However, there are many types of epileptic seizures, which vary greatly from mental absence to falling to the ground and jerking. Seizures can also be sensory, i.e. the patient smells, hears or sees something that is not there. (epilepsy.com).

Figure 27: An illustration of a tonic clonic seizure, in which the body alternates between rigidity and jerking movements (Epilepsy.com).

A patient is diagnosed with epilepsy after recurrent unprovoked seizures. The exact number of seizures that would result in the diagnosis varies. Epilepsy is known to be the most common serious neurological disorder (Perks *et al.* 2012). It affects the patients quality of life, causes injuries and can also be lethal.

Research into epilepsy as well as other neuronal diseases has been mostly focused on ion channels and their ligands (neurotransmitters). Despite the amount of research done around the globe every year on epilepsy and the funds exhausted in the cause, the disorder remains till today very much a black box. Drugs for epilepsy are mainly found through screening programs for substances with anti-seizure effects, such as the one run by National Institute of Neurological Disorders and Stroke (Ninds.com).

With the emergence of the soliton model, it is incumbent on us to investigate which role lipids play in neurological disorders. In this chapter we try to string together pieces of evidence that point to a lipid-related mechanism of epilepsy. The underlying basis for this argument is the relationship between anaesthetics, epilepsy and convulsions;

however we also discuss recent studies that have linked ceramide synthesis with the occurrence of epilepsy.

4.1 What is anaesthetic and what is anticonvulsant?

Anticonvulsants are drugs that are used to treat epileptic seizures. They are a very diverse group with varying chemical structures. Although anticonvulsants are clinically categorised as a class of drugs by themselves, they seem to be closely linked with sedatives and anaesthetics. Some common side effects of anticonvulsants are sedation, ataxia (lack of control of bodily movements), lethargy and cognitive impairment (Spiller 1996; Swann 2001; Bradley 2004). Like anaesthetics, anticonvulsants "block" the nerve impulse (Seeman 1972). Moreover, studies have shown that the anticonvulsant dose needed to prevent drug induced seizures in mice correlate strongly with its partition (abbott & acheampong 1988). In a homolougous series, the anticonvulsant potency was found to increase with chain length (Chapman *et al.* 1983).

In addition to anticonvulsants, epilepsy can also be treated with a ketogenic diet, a high fat and low crabohyrate diet. This diet induces a state known as ketosis, where levels of ketone bodies in the blood are elevated. Ketone bodies are produced in order to provide the brain with an energy source in the absence of sugar. In a normal non-dieting individual, the brain only uses glucose as an energy source as fats cannot cross the blood-brain barrier. When fasting or dieting, the liver converts body or diet fats into ketone bodies, which are able to enter the brain. Two of the three ketone bodies, β-hydroxybutyric Acid and acetone have been shown to induce anaesthesia in tadpoles (Yang *et al.* 2007).

On the other hand, anaesthetics are used clinically as a final line of treatment for generalised convulsive status epilepticus. The dose used is only enough to cause sedation without inducing general anaesthesia. (Kälviäinen *et al.* 2005). In cases of patients that are resistant to intravenous drugs, inhaled anaesthetic isoflurane can be used to treat seizures (Hilz *et al.* 1991).

Some anaesthetic and sedatives induce dependence and their withdrawal symptoms vary from delirium and hallucinations to life-endangering convulsive seizures. The most common is alcohol withdrawal (Manasco *et al.* 2012), but benzodiazepine/barbiturate withdrawal is also common (Petursson 1994).

This overlap between anaesthetic and anticonvulsant effects implies that the difference between the two is one of degree rather than category, and the fact that anticonvulsants seem to comply to the Meyer-Overton correlation might indicate that lipids are the action site of anticonvulsants, which in turn would indicate a lipid mechanism for

epilepsy.

4.2 Antagonising anaesthesia

Anaesthetics do not have any neutral antagonists, i.e. substances that inhibit its effect without producing any effects when on their own. Antagonists of the depressant effects of anaesthesia are themselves stimulants of the nervous system (Little 1996).

We have already talked about pressure reversal of anaesthesia, and explained, in section 2.8, that pressure exerts this effect by shifting the melting temperature of lipids upwards. In the absence of anaesthesia, high pressure causes what is known as high-pressure neurological syndrome (HPNS) (Jain 1994). Its symptoms include tremors, jerking, and convulsions. This syndrome is most notably seen in divers. The antagonism between anaesthesia and pressure is utilized to prevent it by mixing nitrogen in breathing air for divers. A study done on crayfish nerves showed that exposure to high pressure resulted in repetitive impulse generation after a single stimulation. Sponatenous impulse generation was also observed. These effects where antagonised by anesthetics (Kendig *et al.* 1978)

Anaesthesia can also be antagonised by chemical substances, which, like high pressure, induce tremors and convulsions. Flumanzenil is probably the only convulsant currently in clinical use. It is used as a waking agent after anaesthesia, and to treat benzodiazepine overdoses (benzodiazepines are used clinically as sedative or anaesthetics) (pro.medicin.dk).

Another notable convulsant is pentylenetetrazole, which is widely used clinically in research for epilepsy mechanism and in researching anti-convulsants. Pentylenetetrazole has been shown to antagonise pentobarbital anaesthesia among other. When applied to single nerves PTZ induces exhibit repetitive impulse generation. Figure 28 shows recordings from our lab done on lobster leg nerve bundle. After immersion in 60 mM PTZ-saline solution, the nerve bundle exhibited repetitive impulse generation after a single stimulation with 400 mV or higher. Picrotoxin and bemegride are also used in epilepsy studies (Langnmen l992)

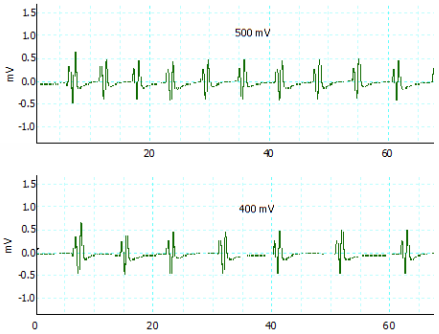

Figure 28: Recording of repetitive impulse firing in lobster leg nerve bundle after immersion in 60 mM pentylenetetrazole for 5 minutes as a response to a 400 mV and 500 mV stimulus. Higher voltages also produces this effect. (Unpublished data).

Despite the antagonism between convulsants and anaesthesia, they do share some properties. Convulsants, like anaesthetics, cause anterograde amnesia and inhibit learn-

ing (Perouansky 2008). Anaesthetics are also known for causing hyperexcitability at the lower concentrations (Little 1996). Some anaesthetics can even cause seizures. Barbiturates which are used clinically as anticonvulsants have been reported to produce varying levels of excitatory effects and rarely generalised seizures. Seizure provocation has also been reported for Nitrous oxide in cats. Local anaesthetics such as lidocaine can also produce convulsions when they cross the blood-brain barrier (Perks *et al.* 2012).

The antagonism between pressure and anaesthesia has been shown, as we reported, to be caused by opposing effects on the melting temperature of lipids. We were not able to find any studies that investigate the effect of convulsatns on lipids. In the next chapter, we investigate the effect of pentylenetetrazole and flurothyl on DMPC vesicles.

4.3 Epilepsy and lipid metabolism

Disorders of lipid biosynthesis affect many physiological functions, one of which is the nervous system, specifically the CNS (Lamari *et al.* 2013). Ceramide synthesis has been especially linked to several neurodegenerative diseases (Ben-David 2010). Although it has been speculated that sphingolipid metabolism is linked to epilepsy, no direct link was found until 2014 when a study found low levels of ceramide synthase 2 (CERS2) in an epilepsy patient (Mosbech *et al.* 2014). Ceramides consist of a sphingosine, which we describe in section 2.3, and a fatty acid. Ceramide is a acetral metabolite in sphingolipid synethesis (Mosbech *et al.* 2014). It had previously been shown that CerS2 mice exhibit abnormal motor function including fast myoclonic jerks and loss of posture lasting 40–60 s (Ben-David *et al.* 2011). The CerS2-null mice also exhibited high sensitivity to audiogenic stimuli.

A study the previous year also done on CerS2-null mice focused on the biophysical properties of brain and liver membranes (Silva *et al.* 2012). By measuring fluorescence anisotropy, they found that lipids extracted from the mice brain showed an increase in the liquid ordered phase and increased segregation between the ordered and disordered phase compared to wild-type mice.

CHAPTER 5

WHAT DO CONVULSANTS DO?

In this chapter, we will investigate the effect of pentylenetetrazole and fluorthyl on DMPC LUVs by measuring their heat capacity using a DSC. We also investigate the joint effect of pentobarbital and pentylenetetrazole.

We chose PTZ because it is commonly used in antagonism studies with anaesthesia, and we chose flurothyl because of its structural relation to halogenated inhaled anesthetics. We also chose these substances because they are readily available compared to much pricier ones such as flumanzenil.

The samples were prepared as described in chapter 3 with a few changes. Since pentylenetetrazole is a powder, we made a stock solution in cholorform. We added the stock solution to the un-hydrated lipid then dried the chloroform off under an air stream. Then it was desiccated in a vacuum chamber for a minimum of 5 hours. Then the sample was hydrated, extruded and degassed as described in chapter..

Flurothyl, on the other hand is a volatile liquid, therefore we added it directly to the sample after preparation and degassing. We did this at 4 °C to avoid evaporation, however, we were later unable to find data on the temperature dependency of flurothyl density, and were forced to use the density at room temperature for calculating the concentrations.

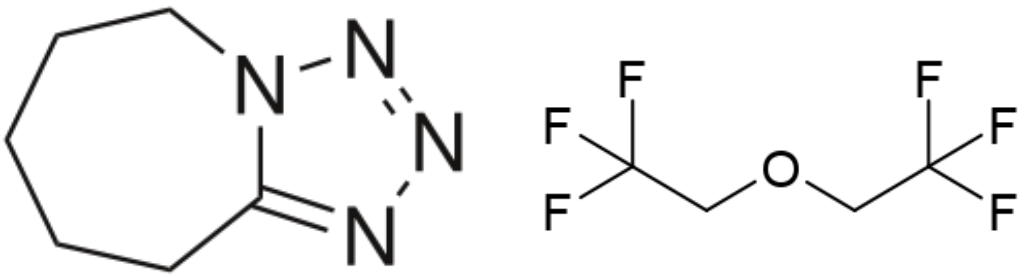

Figure 29: Chemical structures of pentylenetetrazol (left) and flurothyl (right). (wiki commons)

5.1 Results

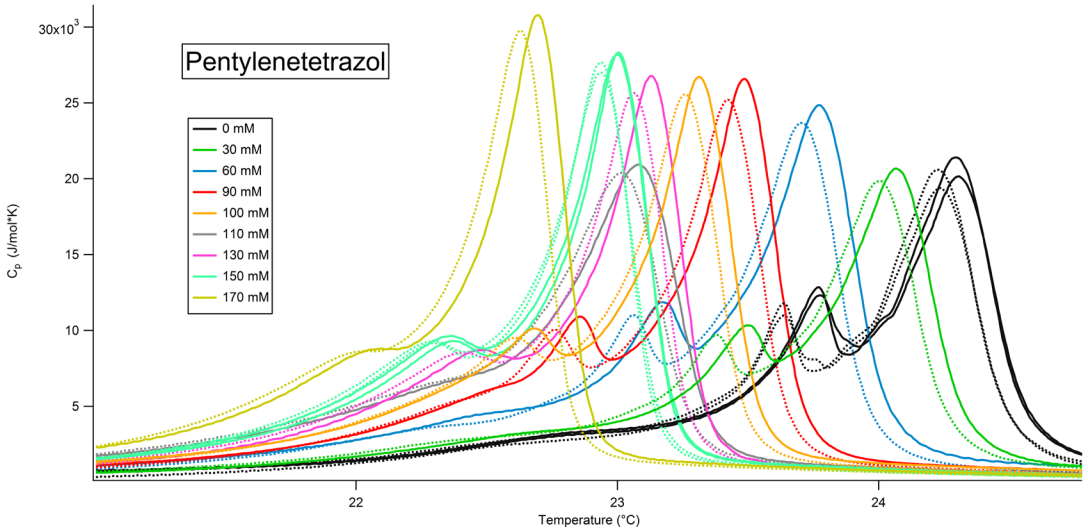

Figure 45: Heat capacity profile of 10 mM DMPC LUV with different concentrations of Pentylenetetrazole.

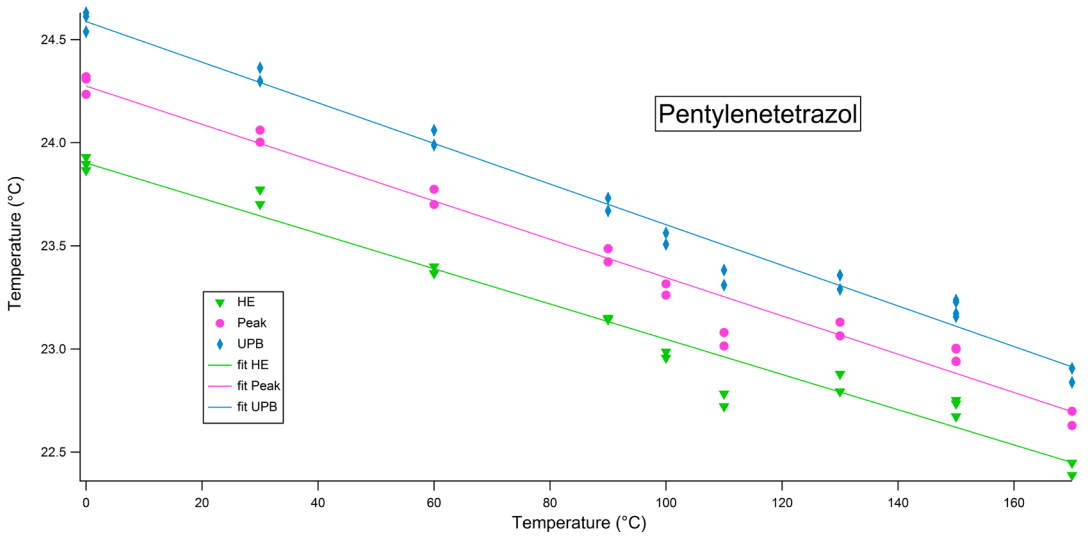

Figure 46: The peak temperatures (T_m)., half enthanlpy temperatures, and upper phase boundary temperatures calculated from the profile in Figure 45

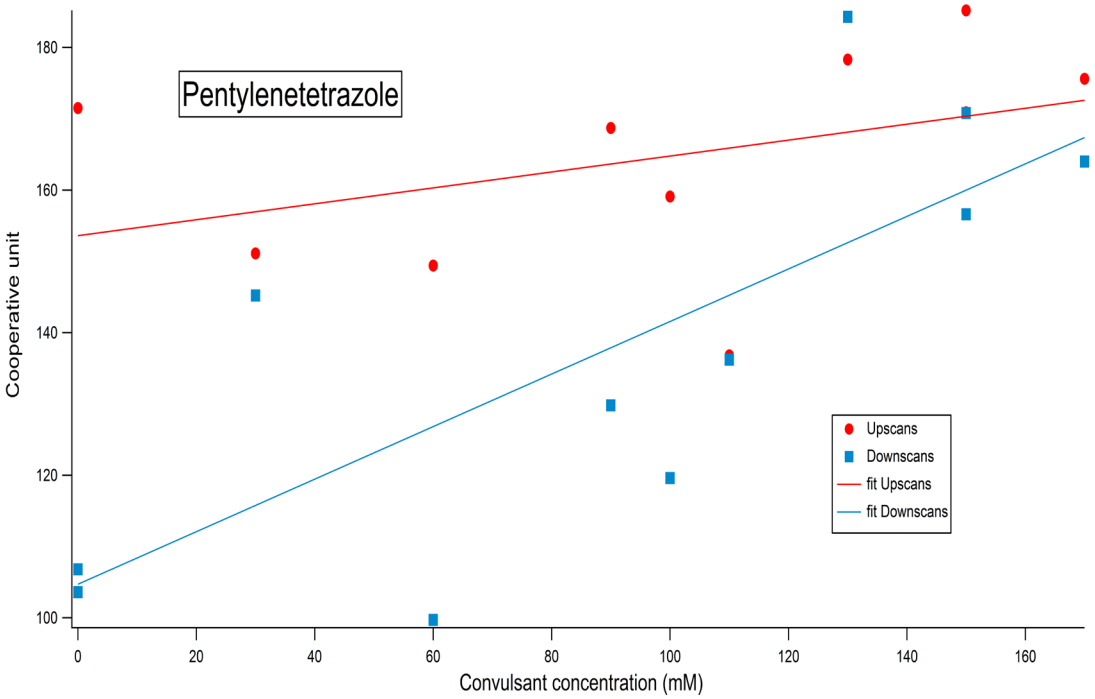

Figure 48: The cooperative unit (a value that reflects the number of molecules that melt cooperatively) calculated from the scans shown in Figure 45.

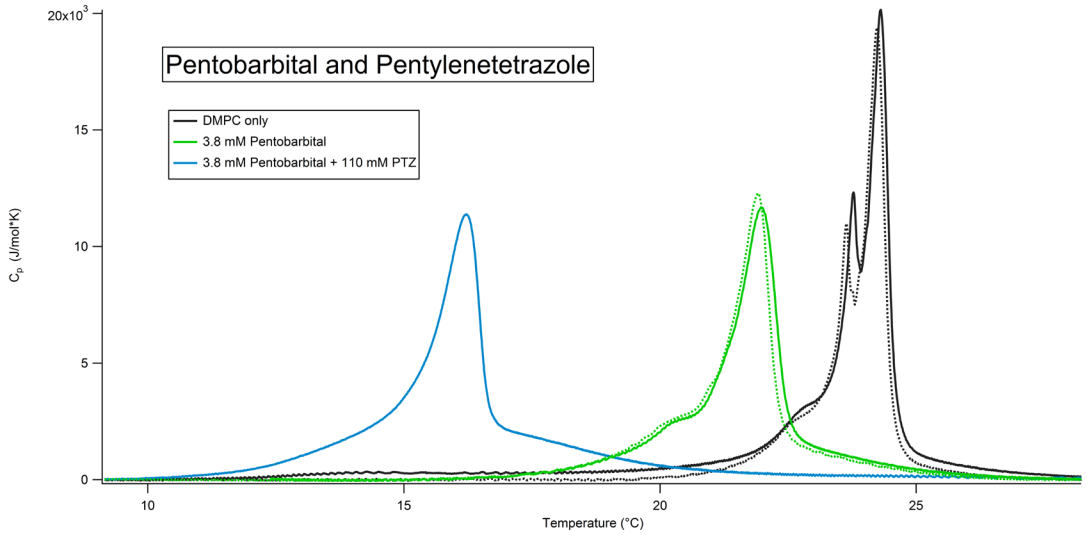

Figure 47: Heat capacity profile of 10 mM DMPC LUV with pentobarbital and with both pentobarbital and pentylenetetrazole.

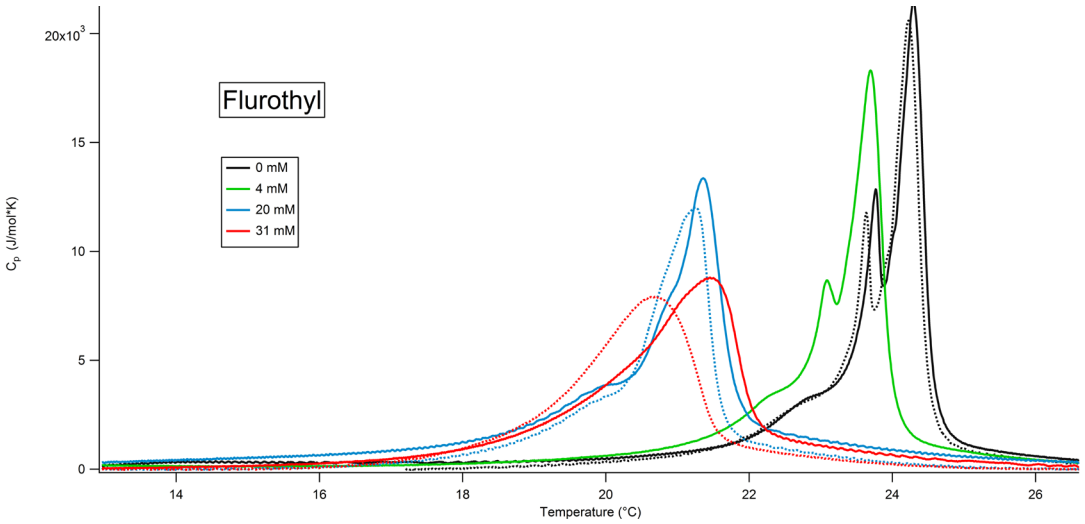

Figure 49: Heat capacity profile of 10 mM DMPC LUV with different concentrations of flurothyl.

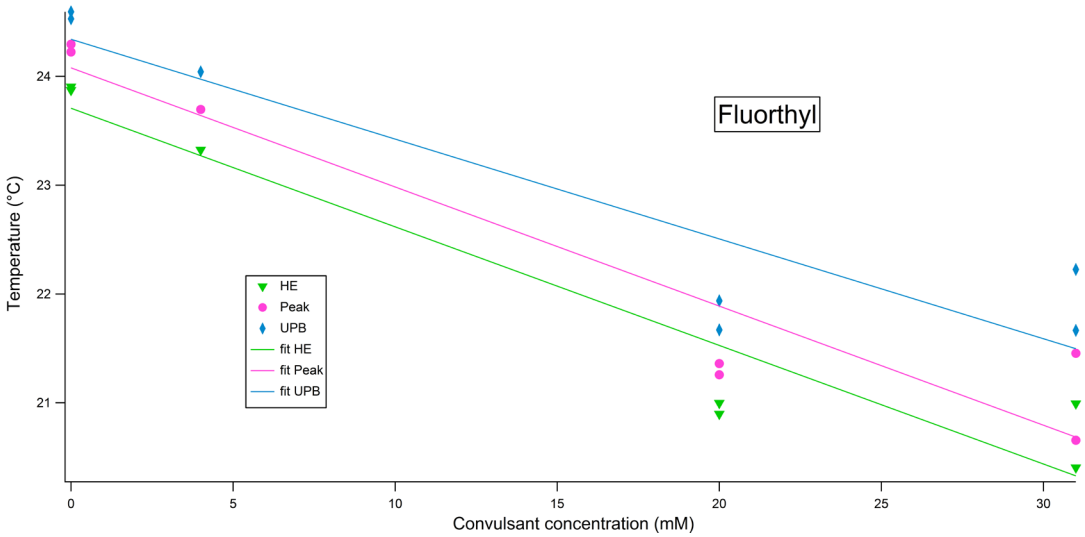

Figure 50: The peak temperatures (T_m)., half enthanlpy temperatures, and upper phase boundary temperatures calculated from the profile in Figure 49.

5.2 Discussion

Although pentylenetetrazole is a convulsant, we see that it has a lowering effect, albeit a weak one, on the melting temperature of DMPC akin to anaesthetics. The weakness of the effect agrees with the fact that Pentylenetetrazole has a low partition coefficient. The melting temperature regresses linearly with the increase in concentration. Pentylenetetrazole does however differ from the anaesthetics we have seen in that in does not broaden the phase transition, but rather makes it narrower. This might be relevant for the formation of solitons in the membrane, since a narrower phase transition means that the number of molecules that undergo cooperative melting is higher. The module that we used for the data analysis included a calculation of copperativity unit. The values calculated for the different heat capacity profiles show a regular increase with the concentration of pentylenetetrazole (Figure 48).

However, when we tested the joint effect of pentylenetetrazole and pentobarbital, we found that pentylenetetrazole lowers the melting temperature even more than when it's acting on its own and moreover, it does not narrow the heat capacity profile.

As for flurothyl, its effect on the phase transition and the melting temperature are exactly like that of anaesthetics. When the melting temperature is plotted against the concentration, it shows a linear regression.

These results seem to disagree with a lipid acting site for pentylenetetrazole and flurothyl's convulsant activity. However, considering the fact that anaesthetics, which lower the melting temperature of artificial phospholids in the lab, do sometimes produce convulsions may indicate that the effect of a substance can depend on the lipid composition. Considering that, we decided to test the effect of anaesthetics and convulsants on biological samples; more specifically, sheep spinal cord.

CHAPTER 6

SPINAL CORD EXPERIMENTS

6.1 Materials and methods

The spinal cord sample was purchased from a local butcher three days after the sheep was slaughtered. It was transported to the laboratory while kept on ice inside a cooler. The spinal column was dissected using a saw and scissors. Throughout this procedure, we took care not to rupture the spinal cord, so that it does not get contaminated with the muscle and bone tissue, and achieved this successfully. The spinal cord was tethered to the bone with connective tissue which we had to sever carefully in order to take out the cord. (Figure 51)

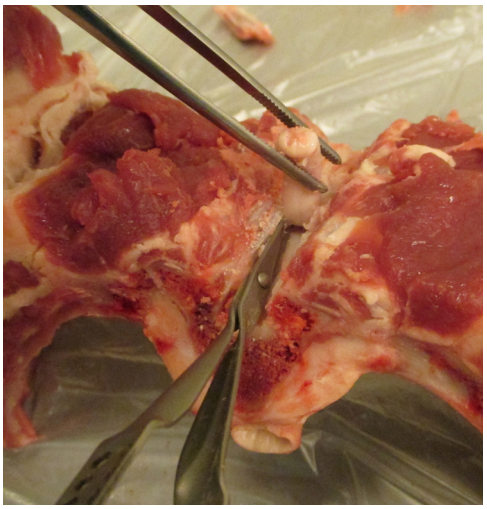

Figure 51: Cutting connective tissue that tethers the spinal cord to the vertebrate column.

After this, we washed the cord from the blood and bone tissue that was on it. Then using a clean pair of scissors and tweezers, we cut the cord vertically, then removed the dura mater which surrounds brain and spinal cord (Figure 52). Then we proceeded to cut it into small pieces to ease the homogenisation process. The pieces were put in a glass bottle, and buffer was added gradually as we homogenised the tissue with the stator rotor.(figure..) This was done with the bottle kept on ice, so as to keep the sample from being heated up. We homogenised in 30 second intervals with 30 second breaks in between. Then the homogenate was decanted into 4 conical tunbes. The glass was washed with a few millilitres of buffer, and this was also added to the tubes. Each tube was filled up to a total of 14 ml.

Figure 52: Removing the dura mater.

Buffer used in these experiments contained 1 mM Hepes, 2 mM EDTA and 150 mM NaCl and was adjusted for pH = 7.42 using NaOH and HCl. We use

more EDTA for the biological samples because they contain enzymes that, when active, would metabolise the lipids and change the membrane properties.

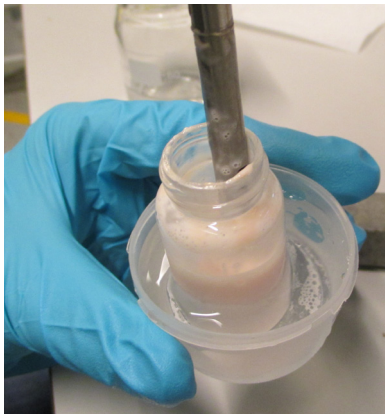

Figure 53: Homogonising the spinal cord with a stator-rotor while kept on icey water.

We centrifuged the sample at about 3360 x g for 15 minutes. This resulted in a liquid but very viscous white pellet and a turbid supernatant. The supernatant was removed and discarded. The tubes were filled up again, then centrifuged again for at the same speed and for the same time interval. Then the supernatant was removed. This was repeated several times until the supernatant was completely clear. The volume of the pellet decreased significantly throughout this process.

We often found fiberous tissue sedemeted at the bottom of the tube. To get rid of it, we decanted the homogenate to a new tube leaving the fiberous tissue stuck to the bottom of the old tube. However, we could see that tiny pieces of fiberous tissue were always present in our samples. This can be problematic, as these pieces would sediment inside the calorimeter cell which would affect its measurements.

Each spinal cord gave us several millimetres of pellet after centrifugation. So we were able to make several samples for calorimeter scanning. For each sample we transferred 1 ml of pellet to a small flask, then the sample was degassed together with the buffer for 10 minutes before adding them to the calorimeter cells.

To add pentobarbital to the samples, we made a stock solution in methanol. We added the required amount into a sample flask, then dried it under an air stream, and put it in the vacuum chamber for 3 hours. Then 1 ml of spinal cord pellet was added and the sample was vortexed in order to dissolve the pentobarbital.

Flurothyl is fluid in room temperature; therefore we added it to the sample using a transferpettor. The sample was degassed before adding flurothyl and was not degassed after, as flurothyl is volatile.

The biological samples were prone to form air bubbles, which we had to avoid as best as possible when filling the sample into the calorimeter with a syringe.

Cleaning the calorimeter after scanning a sample that contains a high protein content was very time consuming, and we had to try several different methods before arriving at one that worked. The reason behind this is the tendency of denatured proteins to adsorb to surfaces. Ethanol might actually aid this adsorption process; therefore we completely skipped it in our cleaning procedure. Instead, we cleaned the cells with mucasol, a detergent, then with water. Then the cell is filled with concentrated HCl and is left to soak in the acid for one hour at 40 °C. Then the cell is cleaned with water using the syringe. And finally, it is cleaned with water using the cleaning devise for half an hour. It is important

to clean thoroughly with water after cleaning with acid, as a low pH would denaturate proteins in the next sample.

To test the cleanliness of the calorimeter, we found it useful to perform a scan with only buffer in both cells.

6.2 Results

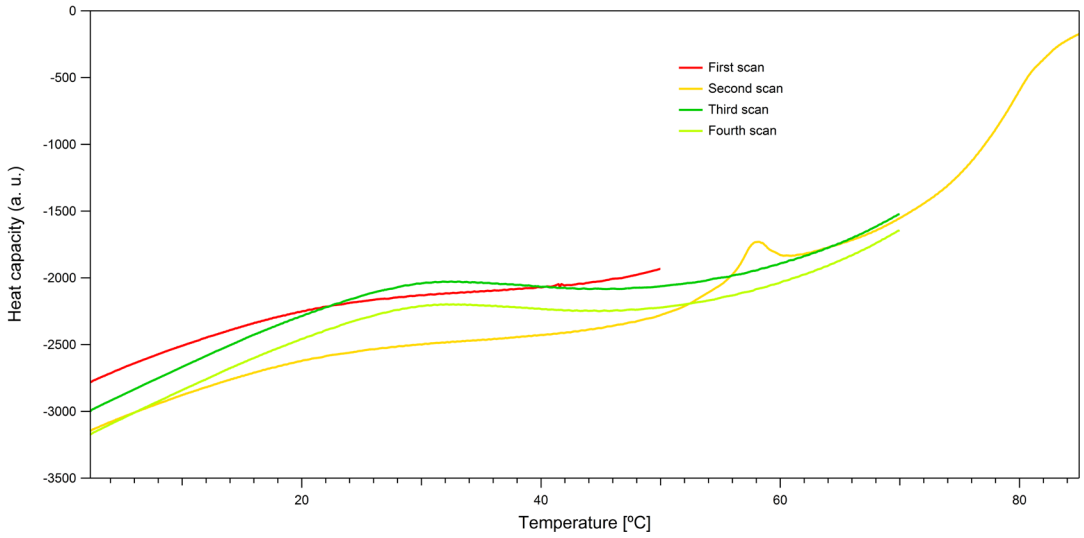

Figure 54: Four upscans of the same spinal cord sample. The first scan was from 1 °C to 45 °C. The second from 1 °C to 85 °C. The third and fourth from 1 °C to 70 °C.

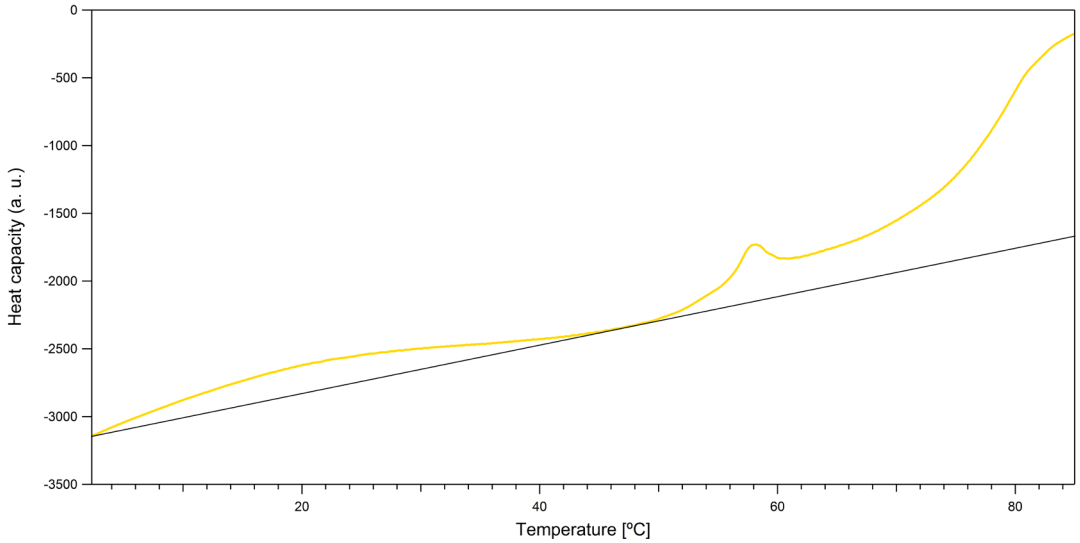

Figure 55: The first scan from Figure 54. Here, we illustrate the baseline substration that we tried using on our samples.

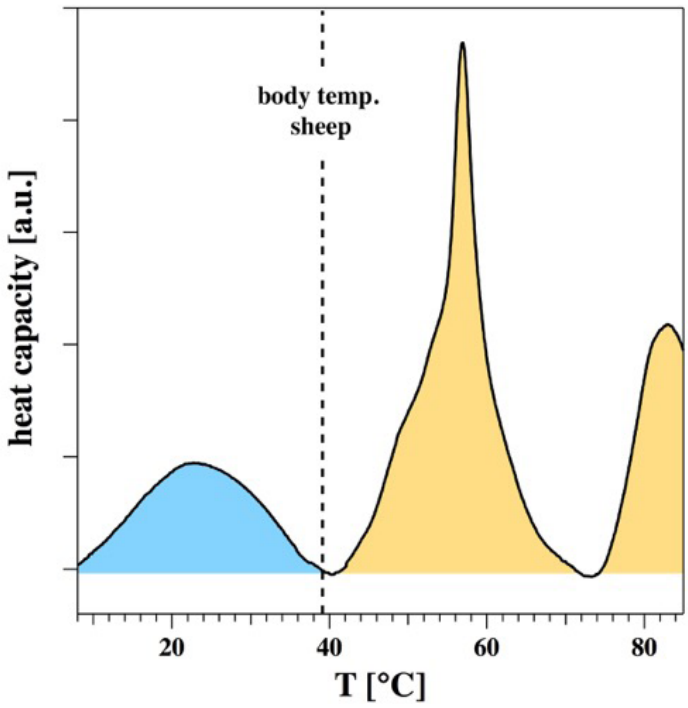

Figure 56: This figure was obtained by substracting a linear baseline from one of the ours cpinal cord sample scans (raw data not shown) using the method illustrated in Figure 55.

6.3 Discussion

When we obtained our first sucessful scan of a spinal cord sample, we substracted a linear baseline as shown in Figure 55 and got the result shown in Figure 56. Looking at both the raw scan and the analysed one that there is a phase transition that ends excactly at the body temperature of sheep. The consecutive scans in Figure 54 show a reversibility for this transition unlike the one above the body temperature. This indicates that it is a lipid phase transition, while the process seen above the body temperature is protein denaturation (an irriversible process).

When we got further results from other samples, we found that a linear baseline drawn in the way we illustrated might not be a correct one. It is problematic that the phase transition starts at or below 0 °C. The fact that we cannot see any baseline before the phase transition makes data analysis very difficult. Also the fact that the phase transition is a very broad one makes it very difficult to tell whether any changes occured We tried adding pentobarbital and flurothyl in different concentartions to some of the samples, however, we were not able to draw any conclusions from the resulting scans.

To fix this problem, we need to scan from below 0 °C. This can be dangerous both for the calorimeter because of the pressure exerted on it by the expansion of freezing water. Therefore, it is necessary to add an antifreeze agent such as glycerol to the buffer.

There were also other problems with the method we used. The samples we got had a high content of non-lipid materials, therefore we had to work with a very thick and viscous sample in order to see the lipid signal. When the sample is diluted, noise increases greatly, unless the scanning rate in increase to 40 °C/min. We suspect that a lot of the material present in the samples is extracellular matrix proteins. To test this, we propose incubating the sample with collagenase before centrifugation. This enzyme specifcally targets collagenase, one of the major components of the extracelluar matrix. When digested into smaller pieces, the protein structure would not sedement in the centrifgue. It might also be help to filter the homogenate before centrifugation to get rid of fiberous tissue.

One might also consider using lobster nerves rather than spinal cord, as it is possible to obtain lobster nerves without any connective tissue. Thus one would be testing the effect of the drugs on excitable membranes only rather than a mixture of the membranes of all the cell types present in the central nervous system.

PERSPECTIVE AND OUTLOOK

In this project we found that the soliton model adequately explains the cut-off in anaesthetic effect in n-alkanes. However, we were not able to find an explanation for the antagonism between anaesthetics and convulsants. It is possible that in order to find an answer for this question, we need to look at the compositionally intricate biological membranes rather than the simple synthetic phospholipid vesicles.

We also outline facts and findings that point towards a lipid-related mechanism for one of the most prevalent neurological diseases, namely epilepsy. In conclusion, we would like to suggest that alcohol and barbiturate adaptation and withdrawal may provide a simple way to study the possible mechanisms of epilepsy. As we pointed out earlier, symptoms of withdrawal from these substances include tremours and convulsions. Inducing withdrawal in model organisms would be easier and cheaper than the genetic studies we discussed.

Finally, we hope that the soliton model will be used to its fullest potential in the quest to understand neurological diseases and how to treat them.

REFERENCE LIST

Abbott, F. S. and A. A. Acheampong (1988). "Quantitative structure- anticonvulsant activity relationships of valproic acid, related carboxylic acids and tetrazoles." Neuropharmacology 27(3): 287.

Allada, A. R. and A. H. Nash (1993). "Drosophila melanogaster as a Model for Study of General Anesthesia: The Quantitative Response to Clinical Anesthetics and Alkanes." Anesthesia & Analgesia 77(1): 19-26.

Antognini, J. F. (2003). Neural mechanisms of anesthesia. Totowa, N.J, Humana.

Anton, A. B., Ai; Nicholls, Ch (1992). "The Anesthetic Effect of Alcohols and Alkanes In Caenorhabditis-elegans (ce)." Research Communications In Chemical Pathology And Pharmacology 78(1): 69-83.

Ben-David, O. and A. Futerman (2010). "The Role of the Ceramide Acyl Chain Length in Neurodegeneration: Involvement of Ceramide Synthases." Neuromol Med 12(4): 341-350.

Ben-David, O., et al. (2011). "Encephalopathy caused by ablation of very long acyl chain ceramide synthesis may be largely due to reduced galactosylceramide levels." The Journal of biological chemistry 286(34): 30022.

Chapman, A. G., et al. (1983). "Acute anticonvulsant activity of structural analogues of valproic acid and changes in brain GABA and aspartate content." Life sciences 32(17): 2023.

Davy, H. S. (1800). Researches, chemical and philosophical, chiefly concerning nitrous oxide, or dephlogisticated nitrous air, and its respiration. By Humphry Davy. London, printed for J. Johnson. By Biggs and Cottle, Bristol.

Edel, C. N. (2015). Molecular and Cellular Physiology of Neurons. Cambridge, Mass. u.a, Harvard University Press.

EN, K. J. S. T. C. (1978). "Anesthetics inhibit pressure-induced repetitive impulse generation." J Appl Physiol Respir Environ Exerc Physiol. 45(5): 747-750.

Engelke, M., et al. (1997). "Effect of inhalation anaesthetics on the phase behaviour, permeability and order of phosphatidylcholine bilayers." Biophysical chemistry 67(1-3): 127.

Erwin, N. and S. Bert (1976). "Single- channel currents recorded from membrane of denervated frog muscle fibres." Nature 260(5554): 799.

Franks, N. L., Wr (1994). "Molecular And Cellular Mechanisms Of General-anesthesia." Nature 367(6464): 607-614.

Franks, N. P. and W. R. Lieb (1985). "Mapping of general anaesthetic target sites provides a molecular basis for cutoff effects." Nature 316(6026): 349.

Frye, L. E., M (1970). "Rapid Intermixing Of Cell Surface Antigens After Formation Of Mouse-human Heterokaryons." Journal Of Cell Science 7(2): 319-&.

Gallaher, J., et al. (2010). "Ion- channel- like behavior in lipid bilayer membranes at the melting transition." Physical review. E, Statistical, nonlinear, and soft matter physics 81(6 Pt 1): 061925.

Graesboll, K., et al. (2014). "The Thermodynamics of General and Local Anesthesia." Biophysical Journal 106(10): 2143.

Hammond, C. C. (2015). Cellular and molecular neurophysiology. Amsterdam, Academic Press.

Hata, T., et al. (2000). "Effect of local anesthetics on the bilayer membrane of dipalmitoylphosphatidylcholine: interdigitation of lipid bilayer and vesicle- micelle transition." Biophysical chemistry 87(1): 25.

Haydon, D. and B. Hendry (1982). "Nerve impulse blockage in squid axons by n- alkanes: the effect of axon diameter." Journal of Physiology (London) 333(1): 393-403.

Heimburg, T. (2005). Thermal biophysics of membranes. Weinheim Chichester. Weinheim, Wiley-VCH : John Wiley distributor.

Heimburg, T. and A. D. Jackson (2007). "The thermodynamics of general anesthesia." Biophysical Journal 92(9): 3159-3165.

Heimburg, T., et al. (2005). "On Soliton Propagation in Biomembranes and Nerves." Proceedings of the National Academy of Sciences of the United States of America 102(28): 9790-9795.

Hilz, M., et al. (1992). "Isoflurane anaesthesia in the treatment of convulsive status epilepticus." J Neurol 239(3): 135-137.

Iwasa, K., et al. (1980). "Swelling of nerve fibers associated with action potentials." Science (New York, N.Y.) 210(4467): 338.

Iwasa, K., et al. (1980). "Swelling of nerve fibers associated with action potentials." Science (New York, N.Y.) 210(4467): 338.

Johnston, D. (1995). Foundations of cellular neurophysiology. Cambridge, Mass, MIT Press.

Kälviäinen, R., et al. (2005). "Refractory Generalised Convulsive Status Epilepticus." CNS Drugs 19(9): 759-768.

Kaminoh, Y., et al. (1992). "Alcohol interaction with high entropy states of macromolecules: Critical temperature hypothesis for anesthesia cutoff." Biochimica et Biophysica Acta - Biomembranes 1106(2): 335-343.

Kassahun, B. T., et al. (2010). "A Thermodynamic Mechanism Behind an Action Potential and Behind Anesthesia." Biophysical Reviews and Letters 05(01): 35-41

Keynes, R. D. (2011). Nerve and Muscle. Cambridge, Cambridge University Press.

KK., J. (1994). "High-pressure neurological syndrome (HPNS)." Acta Neurol Scand 90(1): 45-50.

Lamari, F., et al. (2013). "Disorders of phospholipids, sphingolipids and fatty acids biosynthesis: toward a new category of inherited metabolic diseases." Official Journal of the Society for the Study of Inborn Errors of Metabolism 36(3): 411-425.

Langmoen, I. A., et al. (1992). "An experimental study of the effect of isoflurane on epileptiform bursts." Epilepsy research 11(3): 153.

Lever, M. J., et al. (1971). "Pressure Reversal of Anaesthesia." Nature 231(5302): 368.

Little, H. (1996). How has molecular pharmacology contributed to our understanding of the mechanism(s) of general anesthesia? Pharmacol. Ther. 69: 37-58.

Loeb, J. (1904). "THE RECENT DEVELOPMENT OF BIOLOGY." Science (New York, N.Y.) 20(519): 777.

Madsen, S. B. (2012). "Thermodynamics of nerves." Master thesis. can be obtained on membranes.nbi.dk

Manasco, A., et al. (2012). "Alcohol withdrawal." Southern medical journal 105(11): 607.

Meyer, H. (1901). "Zur Theorie der Alkoholnarkose." Archiv f. experiment. Pathol. u. Pharmakol 46(5): 338-346.

Miller, K. (1977). "Opposing Physiological-effects of High-pressures And Inert-gases." Federation Proceedings 36 (5): 1663-1667.

Miller, R. D. (2005). Miller's Anesthesia. New York, Churchill Livingstone.

Morgulis, S. (1935). "The Theory of Narcosis: III. (Biochem. Zeitschr., vol. cclxxvii, pp. 39-71, 1935, cf. C.A., vol. xvii, p. 2917.) Meyer, K. H., and Hemmi, H." The British Journal of Psychiatry 81(335): 959-959.

Mosbech, M. b., et al. (2014). "Reduced ceramide synthase 2 activity causes progressive myoclonic epilepsy." Annals of Clinical and Translational Neurology 1(2): 88-98.

Overton, C. E. (1901). Studien über die Narkose zugleich ein Beitrag zur Allgemeinen Pharmakologie, Fischer.

Overton, C. E. (1991). Studies of narcosis. London, United Kingdom, London, New York, Chapman and Hall Ltd and the Wood Library-Museum of Anesthesiology.

Perks, A., et al. (2012). "Anaesthesia and epilepsy." British Journal of Anaesthesia 108(4): 562-571.

Perouansky, M. (2008). "Non- immobilizing inhalational anesthetic- like compounds." Handbook of Experimental Pharmacology 182: 209-223.

Pétursson, H. (1994). "The benzodiazepine withdrawal syndrome." Addiction 89(11): 1455-1459.

Pringle, M. J., et al. (1981). "Can the lipid theories of anesthesia account for the cutoff in anesthetic potency in homologous series of alcohols?" Molecular pharmacology 19(1): 49.

Roth, S. and P. Seeman (1972). "The membrane concentrations of neutral and positive anesthetics (alcohols, chloropromazine, morphine) fit the meyer- overton rule of anesthesia; negative narcotics do not." BBA - Biomembranes 255(1): 207-219.

Seeman, P. (1972). "The membrane actions of anesthetics and tranquilizers." Pharmacological reviews 24(4): 583.

Shafer, S. L. and D. R. Stanski (2008). "Defining depth of anesthesia." Handbook of Experimental Pharmacology 182: 409-423.

Silva, L. C., et al. (2012). "Ablation of ceramide synthase 2 strongly affects biophysical properties of membranes." Journal of lipid research 53(3): 430.

Spiller, H. and G. Bosse (1996). Management of acute anticonvulsant overdose. CNS Drugs. 6: 113-129.

Swann, A. (2001). "Major system toxicities and side effects of anticonvulsants." Journal Of Clinical Psychiatry 62: 16-21.

Tasaki, I., et al. (1969). "Fluorescence changes during conduction in nerves stained with Acridine Orange." Science (New York, N.Y.) 163(3868): 683.

Urban, B. W. (2008). "The site of anesthetic action." Handbook of Experimental Pharmacology 182: 3-29.

Wodzinska, K., et al. (2009). "The thermodynamics of lipid ion channel formation in the absence and presence of anesthetics. BLM experiments and simulations." Soft Matter 5(17): 3319-3330.

Yang, L., et al. (2007). "Anesthetic properties of the ketone bodies beta- hydroxybutyric acid and acetone." Anesthesia and analgesia 105(3): 673.

Yatsu, F. M. (2004). "Neurology in Clinical Practice: The Neurological Disorders, 4th ed." Neurology 62(9): 1657-1657.

Yaws, C. L. (2014). Thermophysical Properties of Chemicals and Hydrocarbons, Gulf Publishing Company.